Design of Rectifier Antenna for Microwave Energy Harvesting Application

HAZEM MOHAMED JAMAL ALLOH

Supervised by

Dr. TALAL SKAIK

A Thesis Submitted in Partial Fulfillment of Requirements for the Degree of Master in Electrical Engineering Communication Systems.

February, 2016

<div dir="rtl">

إقــــــرار

أنا الموقع أدناه مقدم الرسالة التي تحمل العنوان:

</div>

Design of Rectifier Antenna for Microwave Energy Harvesting Application

<div dir="rtl">

تصميم هوائي مع دائرة تقويم لتطبيقات حصاد طاقة الميكروويف

أقر بأن ما اشتملت عليه هذه الرسالة إنما هو نتاج جهدي الخاص، باستثناء ما تمت الإشارة إليه حيثما ورد، وأن هذه الرسالة ككل أو أي جزء منها لم يقدم من قبل الاخرين لنيل درجة أو لقب علمي أو بحثي لدى أي مؤسسة تعليمية أو بحثية أخرى.

</div>

Declaration

I understand the nature of plagiarism, and I am aware of the University's policy on this.

The work provided in this thesis, unless otherwise referenced, is the researcher's own work, and has not been submitted by others elsewhere for any other degree or qualification.

<div dir="rtl">

Student's name:	حازم "محمد جمال" محمد اللوح	اسم الطالب:
Signature:	حازم "محمد جمال" محمد اللوح	التوقيع:
Date:	13/2/2016	التاريخ:

</div>

i

نتيجة الحكم على أطروحة ماجستير

بناءً على موافقة شئون البحث العلمي والدراسات العليا بالجامعة الإسلامية بغزة على تشكيل لجنة الحكم على أطروحة الباحث/ حـازم محمـد جمـال محمـد اللـوح لنيـل درجـة الماجستير فـي كليـة *الهندسـة* قسـم الهندسة الكهربائية – أنظمة الاتصالات وموضوعها:

تصميم هوائي مع دائرة تقويم لتطبيقات حصاد طاقة الميكروويف

Design of Rectifier Antenna for Microwave Energy Harvesting Application

وبعـد المناقشـة التـي تمـت اليـوم السـبت04 جمـادى الأولـى 1437هـ، الموافـق 2016/02/13م الساعة العاشرة صباحاً، اجتمعت لجنة الحكم على الأطروحة والمكونة من:

د. طــــلال فـايز ســـكيك	مشـرفاً و رئيسـاً	
د. عمـار محمـد رمضـان أبـو هـدروس	مناقشـاً داخليـاً	
د. مصـطفى حسـن أبـو نصـر	مناقشـاً خارجيـاً	

وبعد المداولة أوصت اللجنة بمنح الباحث درجة الماجستير في كلية *الهندسة*/ قسم الهندسة الكهربائية – أنظمة الاتصالات.

واللجنة إذ تمنحه هذه الدرجة فإنها توصيه بتقوى الله ولزوم طاعته وأن يسخر علمه في خدمة دينه ووطنه.

والله ولي التوفيق ،،،

نائب الرئيس لشئون البحث العلمي والدراسات العليا

أ.د. عبدالرؤوف علي المناعمة

DEDICATION

To my parents

All I have and will accomplish are only possible due to their love and sacrifices.

To my brothers and sisters

To my Daughter

To my faithful friends

ACKNOWLEDGMENTS

First and foremost, I thank almighty **ALLAH** for giving me the courage and determination, as well as guidance in conducting this research study, deposits all difficulties.

I would like to start out by expressing my deepest gratitude to my advisor, **Dr. Talal Skaik**, for providing me the opportunity to work on this project and for his guidance throughout my research. He is an amazing professor and advisor and it was an honor to work with him.

I am also very grateful to my thesis committee members, **Dr. Ammar Abo Hadrouss** and **Dr. Mustafa Abu Nasr** who reviewed the proposal and development of important notes, cooperation and constructive advices.

My heartiest thanks and deepest appreciation is due to my parents, my brothers and sisters for standing beside me, encouraging and supporting me all the time I have been working on this thesis.

Thanks to all those who assisted me in all terms and helped me to bring out this work.

ABSTRACT

Energy harvesting technology has received a lot of attention as the demand of long life span of energy source increase. Towards that, Rectenna (Rectifier Antenna) or Energy Harvesting system is designed in the current work and it consists of antenna, matching circuit and a rectifier circuit. Microstrip patch antenna where designed to harvest GSM signals. Single-patch antenna and array antennas are designed at 900 MHz for this purpose. The designed antenna has good return loss performance and the array antennas are designed to achieve higher gain and hence more captured energy. The design and optimizing of the performance of the proposed antenna are performed by using Computer Simulation Technology software CST studio design.

The rectifier circuit is a 7 stage voltage doubler circuit using Schottky diodes and it is designed to convert the RF energy into a DC output. A matching circuit has been designed from a single stub to match the complex input impedance of the rectifier circuit to the standard 50 Ω. The design of the rectifier circuits is performed by using NI Multisim 14 software and the output voltage of rectifier was 2.283V.

A single stage rectifier circuit along with matching circuit are fabricated on an FR-4 substrate.

ملخص الرسالة

تكنولوجيا حصاد الطاقة لاقت الكثير من الاهتمام، من حيث زيادة الطلب لإطالة العمر الافتراضي لمصادر الطاقة. لذلك، في هذا المشروع تم تصميم نظام لحصاد الطاقة، وهذا النظام يتكون من ثلاثة دوائر، في الدائرة الأولى تم تصميم هوائي يعمل على تردد شبكات الاتصالات الخلوية الجوال التي تعمل بنظام ال GSM بتردد ٩٠٠ ميجا هيرتز حيث تنبعث من هذا الهوائي طاقة كهرومغناطيسية مترددة صغيرة جدا يمكن استغلالها في حصاد الطاقة ولزيادة هذه الطاقة المنبعثة تم تصميم اثنين من هذه الهوائيات بنظام سلسلة Array للحصول على طاقة منبعثة عالية نوعا ما وتم التصميم باستخدام برنامج المحاكاة الحاسوبي CST microwave studio.

الدائرة الثانية هي عبارة عن دائرة تعديل مع مضاعفة الجهد للطاقة المستقبلة من الهوائي في الدائرة الأولى وتتكون هذه الدائرة من سبع مستويات في كل مستوى تم استخدام اثنين من ثنائيات شوتكي Schottky diode HSMS-2850 حيث تم تحويل طاقة ترددات الراديو المستقبلة الى تيار كهربائي مستمر ومضاعفته سبع مرات بعدد مستويات الدائرة والحصول على جهد يقدر ب 2.283Volts باستخدام برنامج المحاكاة الحاسوبي NI Multisim 14.

الدائرة الثالثة هي عبارة عن دائرة تتوسط الدائرتين السابقتين تسمى دائرة التوافق تعمل على التوفيق ما بين الجهد المستقبل من الهوائي الذي يعمل بنظام ال 50 اوم ودائرة تعديل ومضاعفة الجهد التي تعمل بنظام الجهد الكهربائي وحصد أكبر طاقة ممكنة من خلال تمرير كل الطاقة المستقبلة من الهوائي لدائرة التعديل ومضاعفة الجهد.

في هذا المشروع، عمليا تم تصميم دائرة التوافق مع مستوى واحد من دائرة مضاعفة الجهد لعدم توفر مكونات التصميم في السوق لتصميم الدائرة كاملة ولم نتمكن من اختبارها لعدم توفر أجهزة القياس المراد استخدامها بفعل الحصار والتضييق.

TABLE OF CONTENTS

CHAPTER 1: INTRODUCTION

CHAPTER 2: ANTENNA THEORY

CHAPTER 4: DESIGN OF RECTIFIER ANTENNA

CHAPTER 5: CONCLUSION AND FUTURE WORK

LIST OF TABELS

LIST OF FIGURES

LIST OF ABBREVIATIONS

DC	Direct Current
AC	Alternating Current
RF	Radio Frequency
TV	Television
LAN	Local Area Network
µW	Microwatt
MHz	Megahertz
GHz	Gigahertz
GSM	Global System for Mobile
Ω	Omega in ohm
RFEH	Radio Frequency Energy Harvesting
VHF	Very High Frequency
UHF	Ultra High Frequency
SMS	Short Messaging Service
MMS	Multimedia Messaging Services
PTT	Poste Télécommunications et Télédiffusion
CEPT	Européenne des Postes et Télécommunications
TDMA	Time Division Multiple Access
MoU	Memorandum of Understanding
UL	Up Link
DL	Down Link
MS	Mobile Station
BTS	Base Transceiver Station
EM	ElectroMagnetic
E	Electric fields
H	Magnetic fields
IEEE	Institute of Electrical and Electronics Engineers

dB	decibel
FNBW	First-Null Beam Width
HPBW	Half Power Beam Width
2D	two dimension
3D	third dimension
VSWR	Voltage Standing Wave Ratio
RL	Return Loss
CPS	Coplanar Strip-Line
LED	Light Emitting Diode
DBS	Deep Brain Stimulation
ISM	Industrial Scientific and Medical Band
CST	Computer Simulation Technology

1

Introduction

1.1 Energy Harvesting

The ever increasing use of wireless devices, such as mobile phones, wireless computing and remote sensing has resulted in an increased demand and reliance on the use of batteries. With semiconductor and other technologies continually striving towards lower operating powers, batteries could be replaced by alternative sources, such as Direct Current (DC) power generators employing energy harvesting techniques.

Radio Frequency (RF) energy harvesting, also referred to as RF energy scavenging has been proposed and researched in the 1950s using high power microwave sources, as more of a proof-of-concept rather than a practical energy source, due to the technologies available at the time. However, with modern advances in low power devices the situation has changed with the technique being a viable alternative to batteries in some applications. Particularly, for wireless devices located in sensitive or difficult access environments where battery operated equipment might not have been previously possible [1-2].

In the modern environment there are multiple wireless sources of different frequencies radiating power in all directions. Figure 1.1 shows some that potentially could be exploited for RF energy harvesting applications. These might be, but not limited to; TV and radio broadcasts, mobile phone base stations, mobile phones, wireless Local Area Network (LAN) and radar.
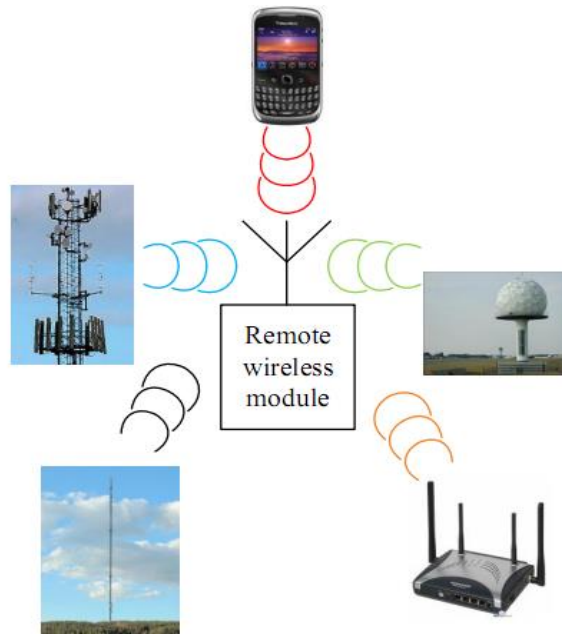
Figure 1.1: Potential RF Harvesting Sources.

The basic energy harvesting system block diagram shown in Figure 1.2, where a transducer typically an antenna or antenna array harvests ambient electromagnetic energy. This harvested energy is rectified and filtered. The recovered direct current (DC) then, either powers a low powered device directly, or stored in a super capacitor for higher power low duty-cycle operation [3].
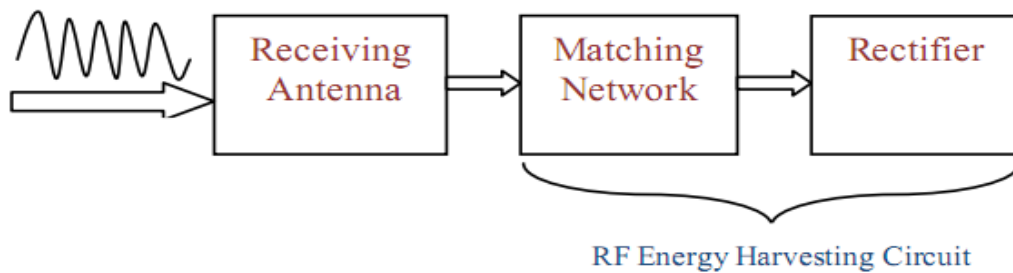
Figure 1.2: Basic RF Energy Harvesting Block Diagram.

RF power source: is generally an antenna which RF signal produces a small sinusoidal voltage. The maximum theoretical power is available for RF power harvesting is 0.7 µW and 1.0 µW for 2.4GHz and 900 MHz frequencies, respectively for free space distance of 40 meter. This research is based on GSM-900, in the 935_960MHz bandwidth.

Impedance matching: the maximum RF power is transferred from source to load by using an input impedance matching circuit. Since the input impedance of the rectifier is different from the RF source (50 Ω), so the impedance matching is needed in case of transferring maximum power.

Rectifier circuit: Rectifier is able to convert an input RF signal into a considerable DC voltage. Due to low power threshold, the efficiency of rectifier is not high enough. Hence one of the challenging parts of designing rectifier is having reasonable efficiency.

The output voltage of rectifier is not stable and consists of ripples. Hence, a low pass filter is needed at the output of circuit to have a constant and smooth DC voltage since most of applications need stable voltage.

The load of rectifier could be a resistor, capacitor, inductor or a combination of all these. In this study, a resistive load is used in simulation.

Frequency selection is an important consideration in RF Energy Harvesting (RFEH) systems and at the same time might be environment specific. As an example for an indoor application wavelength up into the low GHz would be a better choice, due to their ability to propagate well in these environments, rather than lower very high frequency over Ultra High Frequency transmissions VHF/UHF. These might be more useful to outdoor or remote location harvesting applications.

Generally, in the modern built environment Global System for Mobile (GSM) mobile phone signals are prevalent, and propagate well both into and out of buildings, offering harvesting potential from both the GSM base stations as well as the user's handsets.

1.2 Global System for Mobile (GSM)

GSM is the most widely spread mobile communication system all around the world. GSM provides several telecommunications services such as voice calls, data sessions, Short Messaging Service (SMS), Multimedia Messaging Services (MMS), etc. In 1982, the Poste Télécommunications et Télédiffusion (PTT) sent a proposal to Conférence Européenne des Postes et Télécommunications (CEPT) to specify a common European telecommunication service in the 900 MHz band. GSM standardization group was then established to formulate the specifications for this European mobile cellular radio system.

From the year 1982 to 1985, discussions centered around whether to build an analog or a digital system, where GSM decided to develop a digital system. In 1986, companies participated in a field test in Paris to determine whether a narrowband or broadband solution would be deployed. By May 1987, the narrowband Time Division Multiple Access (TDMA) solution was chosen. Concurrently, operators in 13 countries (two operators in the United Kingdom) signed the Memorandum of Understanding (MoU) which committed them to fulfill GSM specifications and deliver a GSM system by July, 1991 [4]. As compared with other technologies, GSM dominates about 80% from the total number of subscribers which is about 4.7 billion subscribers in the second quarter, 2015 [5].

GSM is a system that consists of three subsystems that all make a complete and operational system as will be pointed out in the following sections.

1.3 GSM Physical Bands

GSM 900, GSM 1800 and GSM 1900 are the common three GSM bands. These bands come to fulfill the needs of the increasing number of demanding customers. The most common GSM band is the 900 MHz band which is used in Palestine Cellular Communications Company Jawwal for GSM network. Each band is divided into two sub-bands which are called Up Link (UL) from the Mobile Station (MS) to the BTS and Down Link (DL) from the BTS to the MS. The idea behind this separation is to have two separate frequency bands to provide the user with full duplex communication service. The details of the three common GSM bands are shown in table1.1.

Table 1.1: Various GSM Frequency Bands.

Frequency band (MHz)	UL frequency range (MHz)	DL frequency range (MHz)
GSM 900	890-915	935-960
GSM 1800	1710-1785	1805-1880
GSM 1900	1850-1910	1930-1990
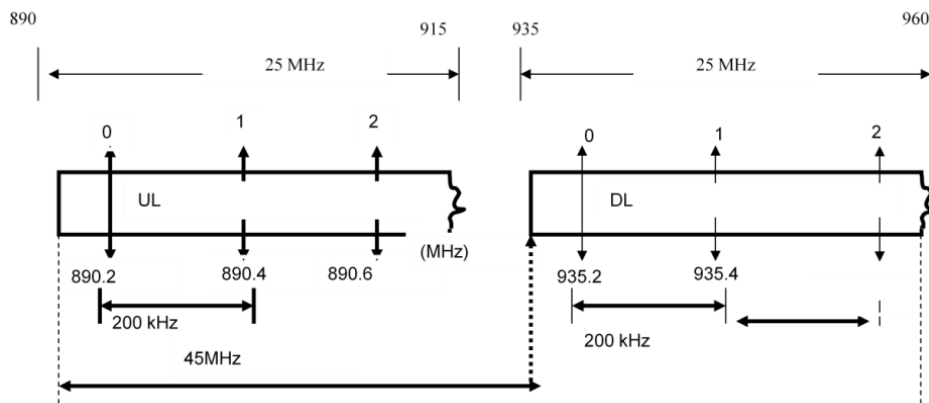
Figure 1.3: GSM 900 Band with UL, DL, Channel Bandwidth and Duplex Distance[6].

1.4 Thesis Objective

The main objective of this project is to design an energy harvesting system consisting of a rectangular microstrip antenna, a matching circuits and rectifier circuit that can capture energy of the available GSM signals and convert it into DC output. The harvesting system has potential application of charging mobile and other equipment.

1.5 Thesis Outline

This thesis is composed of five chapters.

Chapter 1 presents an introduction to the topic and objectives of the project. In Chapter 2, we introduce a background on the antenna basics, Maxwell's equations and the radiation pattern of the antenna. Antenna parameters such as directivity, gain and polarization and microstrip antenna design equations are also discussed. Chapter 3 introduces the rectifier's basics, the type of rectifier, the voltage doublers circuits and specially the schottky diode. In Chapter 4, literature review, the designs and simulations of rectangular patch antenna, matching circuits and rectifier circuits. Finally, the conclusion of the research and the suggestions for future work are presented in chapter 5.

5

References

[1] Brown, W. Mims, J. Heenan, N. "An experimental microwave-powered helicopter" Raytheon Company, Burlington, MA, USA; 1965 IEEE International Record, vol. 13, part 5, pp.225-235.

[2] R. M. Dickinson, "Evaluation of a microwave high-power reception conversion array for wireless power transmission," Jet Propulsion Laboratory, California Institute of Technology, Pasadena, CA, Tech. Memo 33-741, Sept. 1975.

[3] D. Bouchouicha, F. Dupont, M. Latrach, L. Ventura "Ambient RF Energy Harvesting" STMicroelectronics, France, International Conference on Renewable Energies and Power Quality Granada (Spain), March, 2010

[4] T. Rappaport, Wireless Communications: Principles and Practice, second edition, Prentice Hall, p. 5-9, 2001.

[5] World G.S.M. 2016.market data summary from
http://www.gsma.com/mobileeconomy

[6]   Ericsson, "Radio Network Parameters and Cell Design Data for Ericsson'GSM Systems, User Description", Ericsson AB, p. 9-36, 2008.

2

Antenna Theory

2.1 Introduction

An antenna is a passive device to transform an RF signal, traveling on a conductor, into an electromagnetic (EM) guided wave in free space and vice versa [11]. An antenna acts as a transitional structure between the guiding device (e.g. waveguide, transmission line) and the free space. The official IEEE definition of an antenna as given by Stutzman and Thiele [1] follows the concept: "That part of a transmitting or receiving system that is designed to radiate or receive electromagnetic waves "as shown in figure 2.1. When operating as a transmitter, the antenna accepts a wave propagating as a mode along a waveguide or transmission line, and emits a radiating wave into free space. As a receiver, the antenna intercepts a wave in free space and introduces a propagating wave on a transmission line.
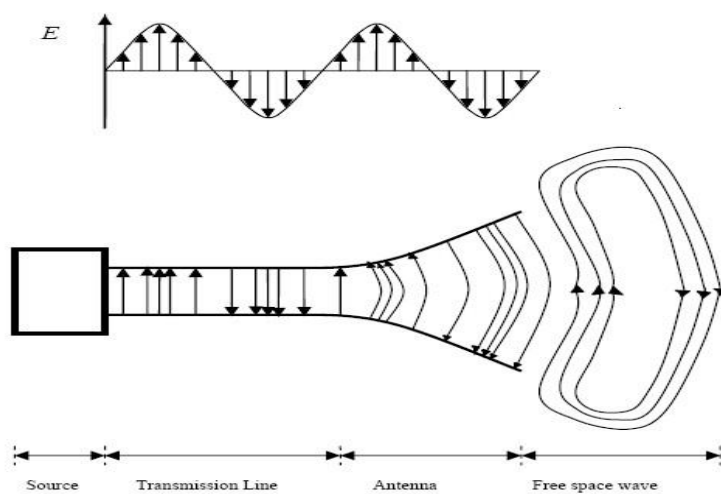
Figure 2.1: Antenna as a transition device.

Antennas are frequency-dependent devices. Since each antenna is designed to operate in a certain frequency band and reject signals from the other operating band, antennas can be considered as a low pass filters.

2.2 Antennas to Radio Waves

James Clerk Maxwell (1831–1879) presented a set of equations named as Maxwell's equations that describe the interrelationship between electric fields E, magnetic fields H, electric charge $\boldsymbol{\rho}$, and current density J [6]. Here we toke one case as a single frequency source case (an arbitrary case can be considered the combination of many single-frequency sources), thus Maxwell's equations can be written as [6]:

$$\nabla \text{ X } \mathbf{E} = -\mathbf{j}\omega\mu \text{ } \mathbf{H} \tag{2.1}$$

$$\nabla \text{ X } \mathbf{H} = \mathbf{J} + \mathbf{j}\omega \text{ } \varepsilon\mathbf{E} \tag{2.2}$$

$$\nabla \cdot \mathbf{E} = \frac{\rho}{\varepsilon} \tag{2.3}$$

$$\nabla \cdot \mathbf{H} = \mathbf{0} \tag{2.4}$$

$\boldsymbol{\rho}$ is the charge density, ω is the angular frequency, μ is a scalar quantity, ε electric permittivity.

$\nabla = \mathbf{i}\frac{\partial}{\partial \text{x}} + \mathbf{j}\frac{\partial}{\partial \text{y}} + \mathbf{k}\frac{\partial}{\partial \text{z}}$ is a vector operator.

From equations listed a new equation can be derived [6]:

$$\nabla^2 E + \omega^2\mu\varepsilon E = \mathbf{j}\boldsymbol{\omega}\mu\mathbf{J} + \nabla(^\rho/_\varepsilon) \tag{2.5}$$

This equation links the radiated electric field (no magnetic field) directly to the source [6]. To solve this equation, boundary conditions are required for an open boundary, so the field disappears when the distance from the source V to the field point becomes infinite, see figure 2.2.
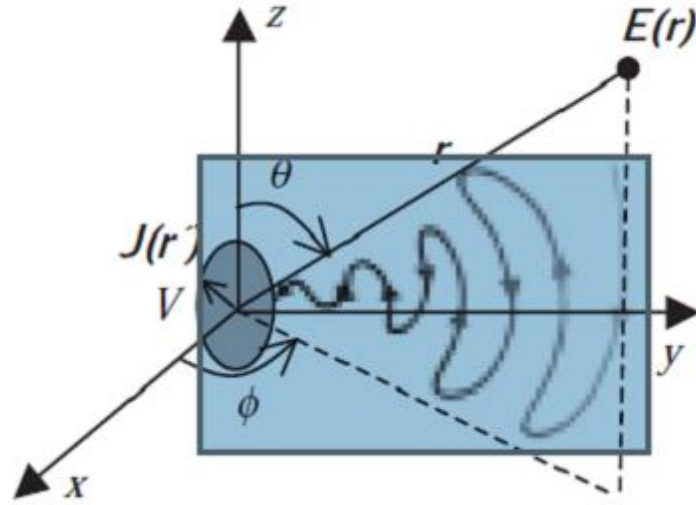
Figure 2.2: Radio waves generated by a time varying source [6].

$$\mathbf{E(r)} = -\mathbf{j\omega\mu} \int_v \mathbf{J}(\acute{r}) \frac{e^{-j\beta.|r-r'|}}{4\pi|r-r'|} \mathbf{d\acute{v}} + \frac{1}{j\omega\varepsilon} \mathbf{\nabla}(\mathbf{\nabla}. \int_v \mathbf{J}(\acute{r}) \frac{e^{-j\beta.|r-r'|}}{4\pi|r-r'|} \mathbf{d\acute{v}}) \qquad (2.6)$$

Equation (2.6) is the solution of Equation (2.5) in a uniformed medium μ and ε, where r is the distance vector from the origin to the observation point and r' is from the origin to the source point [6].

This equation is the most institution of antenna theory, because it shows how the antenna is related to radio waves, and it gives the radiated electric field from a time varying current J (the time factor $e^{j\omega t}$ is omitted here). Only vibrating (time-varying) current charges as shown in Figure 2.2. It can generate a radio wave (not DC current or static charges) [6]. Antenna design is all about how to control the current distribution J and hence to obtain the desired radiated field E. Antenna theory could be summarized by this single complicated equation, which consists of vector partial differentiation and integration [6].

2.3 Near-Field and Far-Fields

Antenna has three regions as seen in figure 2.3. First region is called the Reactive Near-Field Region which is the portion of the nearfield region immediately surrounding the antenna wherein the reactive field (nonradiating field) predominates [6]. For most antennas, the outer boundary of this region exist at a distance (R< $0.62\sqrt{d^3/\lambda}$) from the

9

antenna surface, where λ is the wavelength, and d is the largest dimension of the antenna [1].

The second region is called radiating Near-Field (Fresnel) which is the region of the field of an antenna between the reactive near-field region and the farfield region wherein radiation fields predominate and wherein the angular field distribution is dependent upon the distance from the antenna. If the antenna has a maximum dimension that is not large compared to the wavelength, this region may not exist [6]. The inner boundary is taken to be the distance ($R \geq 0.62\sqrt{d^3/\lambda}$) and the outer boundary the distance ($R < 2d^2/\lambda$) [1]. The third region is called Far-Field (Fraunhofer) and can be defined as the region of the field of an antenna where the angular field distribution is essentially independent of the distance from the antenna [6]. The far-field regions exist at distances ($R > 2d^2/\lambda$) from the antenna [1]. And, $r_1 = 0.62\sqrt{d^3/\lambda}$, $r_2 = 2d^2/\lambda$, see figure (2.3).
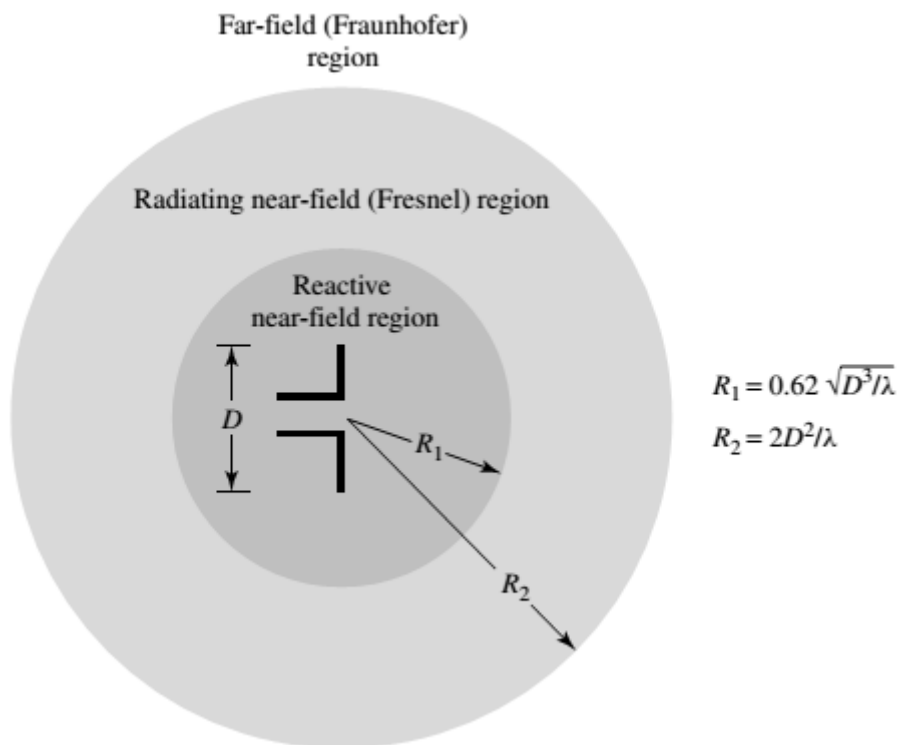
Figure 2.3: Antenna field regions [6].

2.4 Fundamental Parameters of Antenna

Antenna parameters are used to characterize the performance of an antenna when designing and measuring antennas. The most fundamental antenna parameters such as radiation pattern, gain, input impedance, bandwidth and polarization are explained.

2.4.1 Antenna Radiation Patterns

The radiation pattern is defined as a graphical representation of the radiation properties of the antenna as a function of space coordinates, and can be drawn with three-dimensions (3D) [1]. As seen in figure 2.4, the 3D pattern is a good way for the radiated field distribution as a function of angle θ and φ in space. The radiation patterns in the two main planes are the E-plane, and the H-plane. The E-plane belongs to the electric field E plane, and the H-plane belongs to the magnetic field H plane.

In ideal current element case, the electric field is $E\theta$ and the magnetic field is $H\varphi$, so the E-plane pattern is the field $E\theta$ measured as a function of θ when the angle φ and the distance are fixed [6]. The H-plane pattern is the field, $E\theta$ measured as a function of φ when the angle θ and the distance are fixed. It should be pointed out that the radiation patterns in figure 2.4 are plotted on a logarithmic scale (dB plot) that helps us to see details of the field or power over a large dynamic range, especially some minor side lobes [6].

Figure 2.4: coordinate system of antenna analysis

2.4.1.1 Radiation Pattern Lobes

A radiation lobe is a portion of the radiation pattern bounded by regions of relatively weak radiation intensity [12], and [6]. As seen in figure 2.4, and 2.5, radiation pattern can be divided to main lobe, minor lobes, side lobes and back lobes.
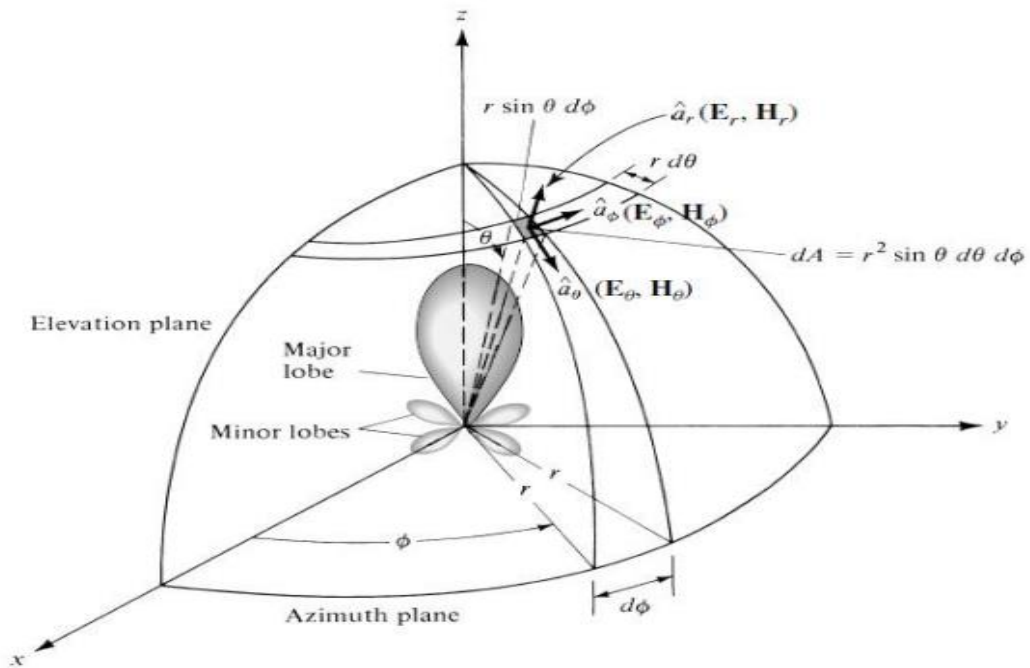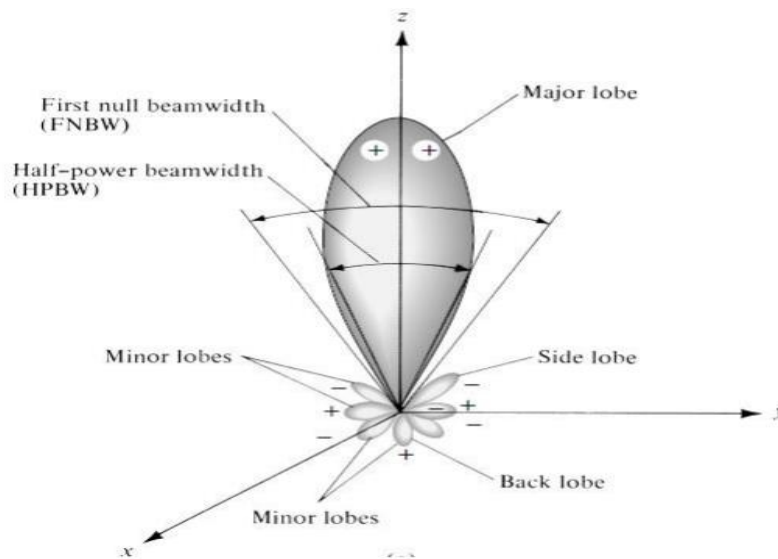

Figure 2.5: radiation pattern lobes 3D [1].

Minor lobes usually represent radiation in undesired directions, and they should be minimized. The Side lobes are the biggest of the minor lobes. The level of minor lobes is defined as a ratio of the power density, often termed the side lobe level [6]. In several radar systems, low side lobe ratios are very important to minimize false target indications through the side lobes [1]. Figure 2.6 describes the radiation pattern lobes with two-dimensions (2D) plot. The most common resolution criterion states that the resolution capability of an antenna to distinguish between two sources is equal to half the first-null beam width (FNBW/2), which is usually used to approximate the HPBW [12], see figure (2.4).
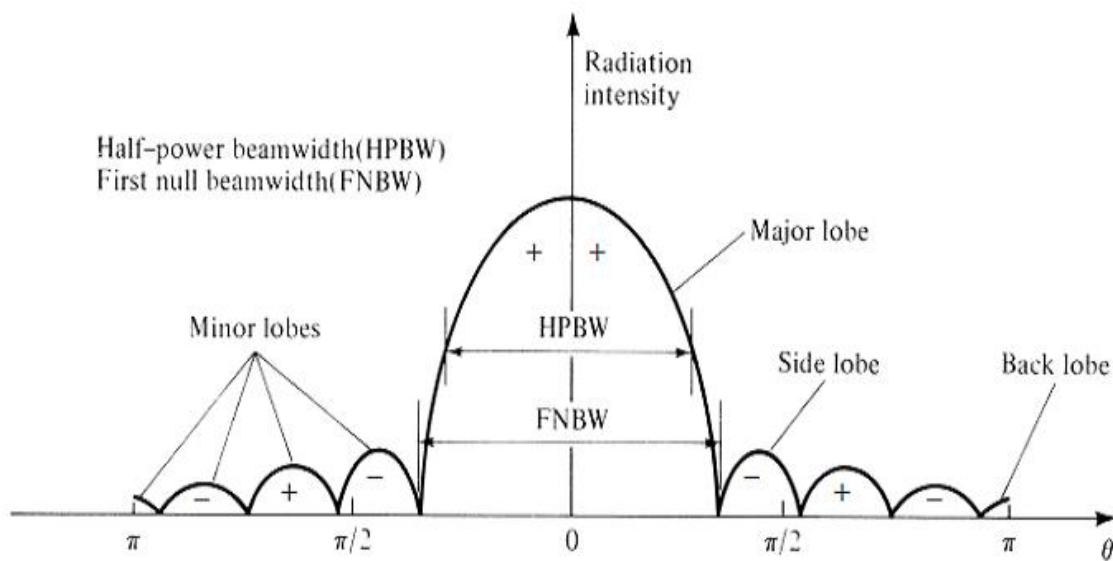
Figure 2.6: 2D radiation pattern lobes [3].

2.4.2 Beam width

The beam width of an antenna is a very important figure and often is used as a trade-off between it and the side lobe level. As seen in figure 2.7 it is also used to describe the resolution capabilities of the antenna to distinguish between two adjacent radiating sources or radar targets [1], and [6]. There are two types of beam width, the first type is called Half-Power Beam Width (HPBW), and it can be defined as the angle between the two directions in which the radiation intensity is one-half value of the beam, or the angular width of the main beam at the half-power points [1]. The second type is called First Null Beam width (FNBW) and it can be defined as an Angular separation between the first nulls of the pattern [1], and [3], see figure 2.7.

(a) Three dimensional   *(b) Two-dimensional*
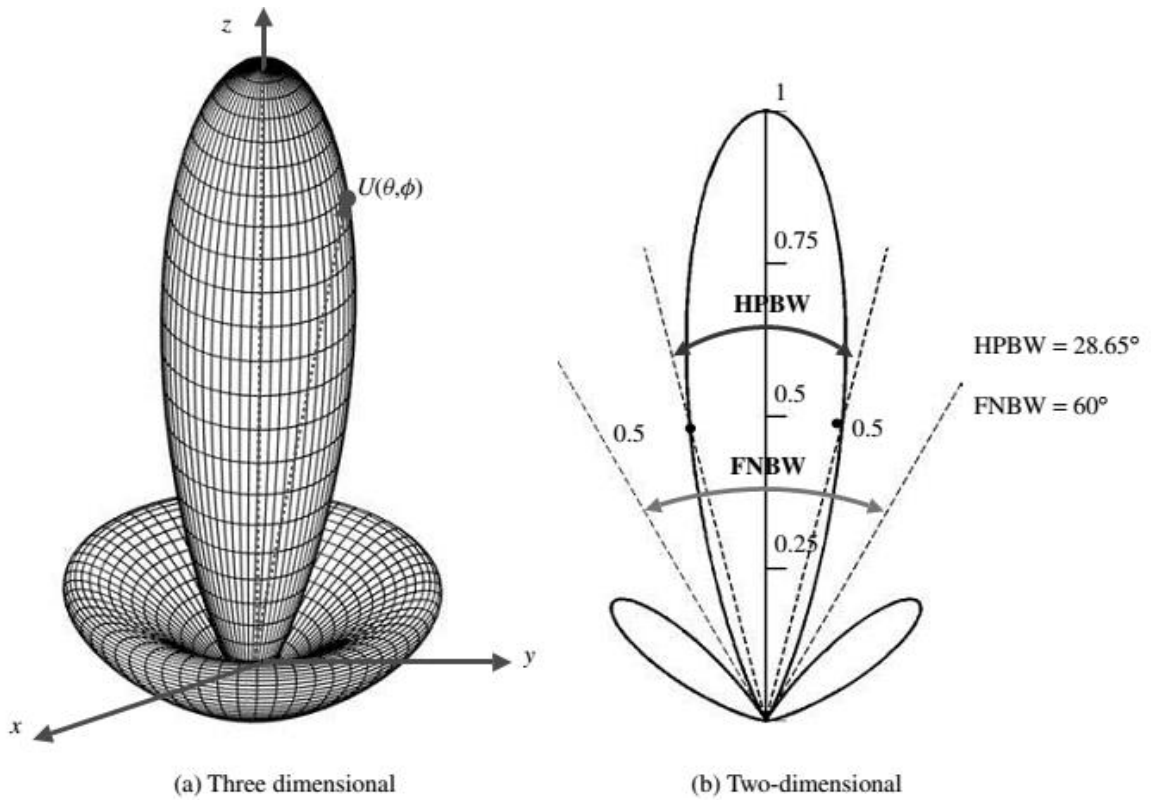
Figure 2.7: 3D and 2D power patterns [1].

2.4.3 Radiation Power Density

First, the radiation density can defined as the power density of an antenna in its far field region. The instantaneous Poynting Vector $\overrightarrow{\mathbf{W}}$ is defined as the quantity used to describe the power associated with an electromagnetic wave [1]:

$$\overrightarrow{\mathbf{W}}= \vec{\mathbf{E}} \; \mathbf{X} \; \overrightarrow{\mathbf{H}} \tag{2.7}$$

$\overrightarrow{\mathbf{W}}$: instantaneous Poynting vector (W/m2)

$\vec{\mathbf{E}}$: instantaneous electric field intensity (V/m)

$\overrightarrow{\mathbf{H}}$: instantaneous magnetic field intensity (A/m)

Since the Poynting vector is a power density, then the total power crossing a closed surface can be obtained by integrating the normal component of the Poynting vector over the entire surface, and be written as [1], and [6]:

14

$$\mathbf{P} = \oiint \mathbf{W} \cdot \vec{n} \, \mathbf{da}. \tag{2.8}$$

where

P = instantaneous total power crossing a closed surface (W).

$\vec{\mathbf{n}}$ = unit vector normal to the surface.

W = instantaneous Poynting vector (W/m^2)

da = infinitesimal area of the closed surface (m^2)

The average power density (time average Poynting vector) can written as [1], [6]:

$$W_{av}(x, y, z) = \widetilde{W}(x,y,z;t)_{av} = [\vec{E} \times \vec{H}^*]/2 \ (W/m^2) \tag{2.9}$$

The real average power density is represented by the real part of $[\vec{E} \times \vec{H}^*]/2$ and the reactive power density is represented by the imaginary part of $[\vec{E} \times \vec{H}^*]/2$ .From (2.9) the average power radiated can be written as [1]:

$$P_{rad} = P_{av} = \oiint_s \vec{W}_{rad} \cdot \mathbf{d\vec{s}} = \oiint_s \mathbf{W} \cdot \vec{n} \quad \mathbf{da} = \frac{1}{2} \oiint_s \mathbf{Re} \oiint_s [\vec{E} \times \vec{H}^*] \cdot \mathbf{d\vec{s}} \tag{2.10}$$

2.4.4 Radiation Intensity

Radiation Intensity is defined as radiated power from any antenna per solid angle (radiated power normalized to a unit sphere) [2], and [1]. The radiation intensity is a far field parameter, so it can be obtained by multiplying the radiation density by the square of the distance.

$$U = r^2 W_{rad} \tag{2.11}$$

where

U=radiation intensity (W/solid angle)

W_{rad} = radiation density (W/m^2)

From (2.11) the power pattern is also a measure of the radiation intensity, so the total power is obtained by integrating the radiation intensity over the entire solid angle of 4π.

$$P_{rad} = \iint_{00}^{2\pi\pi} U(\theta,\varphi) \sin\theta d\theta d\varphi = \iint_{00}^{2\pi\pi} U(\theta,\varphi) \, d\Omega \qquad (2.12)$$

and $d\Omega = \sin\theta d\theta d\varphi$ is defined as the differential solid angle. The radiation intensity of isotropic source is found by dividing the radiation intensity by the area of the unit sphere (4π) which gives [1]:

$$U_0 = \frac{\iint_{00}^{2\pi\pi} U(\theta,\varphi)d\Omega}{4\pi} = \frac{P_{rad}}{4\pi} \qquad (2.13)$$

2.4.5 Directivity

It can be defined as the ratio of the radiation intensity in a given direction from the antenna to the radiation intensity averaged over all directions [1], and [6].

$$D = D(\theta,\varphi) = \frac{U(\theta,\varphi)}{U_0} = 4\pi \frac{U(\theta,\varphi)}{P_{rad}} \qquad (2.14)$$

2.4.5.1 Beam Solid Angle

The beam solid angle (steradian) $\boldsymbol{\Omega_A}$ is define as the solid angle with its vertex at the center of sphere radius r that subtended by a spherical surface area r_2, or can be defined as the solid angle through which all the power of the antenna would flow if its radiation intensity were constant and equal to the maximum value of U for all angles within $\boldsymbol{\Omega_A}$ [1], and [6]. A steradian is a solid angle measurement unit, see figure 2.8. Thus, the directivity can be written as:

$$D = \frac{4\pi}{\Omega_A} \quad \text{and solid angle} \quad \Omega_A = r_2 \sin\theta d\theta d\varphi \qquad (2.15)$$

16
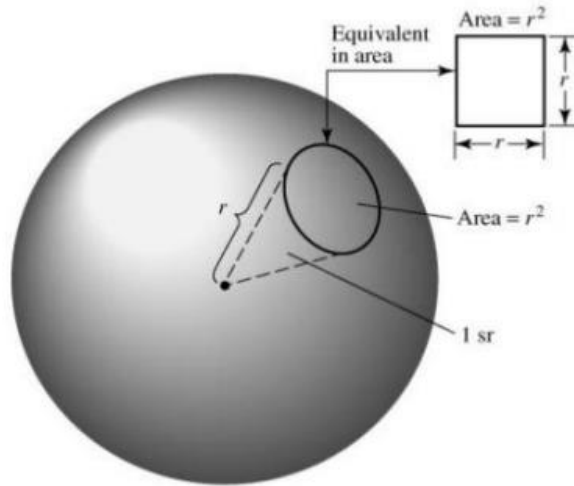
Figure 2.8: Geometrical arrangements for defining a steradian [1].

2.4.6 Antenna Efficiency

The total antenna efficiency e_0 is used to take into account losses at the input terminals and within the structure of the antenna, and e_0 is due to the combination of number of efficiencies [1], see figure2.9.
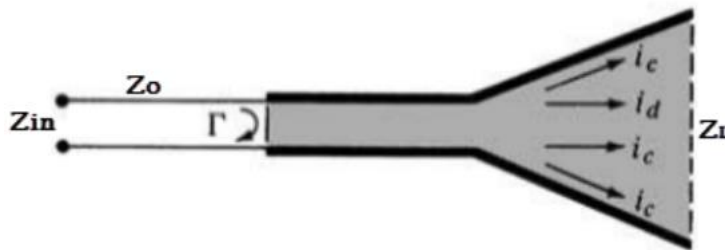
Figure 2.9: Reference terminals and losses of an antenna [1].

The overall efficiency can be expressed as:

$$e_0 = e_r e_c e_d \qquad (2.16)$$

where

e_0 = total efficiency.

e_r = reflection (mismatched with input), $e_r = (1 - |\Gamma|^2)$.

e_c = conduction efficiency.

e_d = dielectric efficiency.

$$\Gamma = \frac{Z_{in}-Z_0}{Z_{in}+Z_0} = \frac{Z_L-Z_0}{Z_L+Z_0} \tag{2.17}$$

$$VSWR = \frac{1+|\Gamma|}{1-|\Gamma|} \tag{2.18}$$

Γ = voltage reflection coefficient at the input terminals of the antenna.

Z_{in} = antenna input impedance.

Z_0 = characteristic impedance of the transmission line.

VSWR =voltage standing wave ratio.

usually e_c and e_d are very difficult to compute, but they can be determined experimentally [1].

2.4.7 Antenna Gain

Antenna Gain is the ratio of the radiation intensity in a given direction to the radiation intensity that would be obtained if the power accepted by the antenna were radiated isotropically [1], and [6]. In addition, the gain of the antenna is related to the directivity.

$$\text{Gain} = 4\pi\frac{radiation\ intensity}{total\ input\ accepted\ power} = 4\pi\frac{U(\theta,\phi)}{P_{in}}\ (dimensionless) \tag{2.18}$$

The antenna gain can be expressed as the ohmic losses (e_{cd})in the antenna multiplied by the antenna directivity $D(\theta, \phi)$.

$$G(\theta, \phi) = e_{cd}\ D(\theta, \phi) \tag{2.19}$$

2.4.8 The Return Loss

The return loss (RL) can be defined by the ratio of the incident power of the antenna P_{inc} to the power reflected back from the antenna of the source P_{ref} [6]. Return loss tells us how much of the input signal is reflected. The Return Loss (RL) may also be explained as the difference between the power of a transmitted signal and the power of the signal reflections caused by variations in link and channel impedance [13], and [14].

Return loss is the negative of the reflection coefficient expressed in decibels. In terms of the voltage standing wave ratio (VSWR). High return loss values mean a close

impedance match, which results in greater differentiation between the powers of transmitted and reflected signals, can be expressed as [6], [13], and [14]:

$$RL = 10 \log_{10} \frac{P_{inc}}{P_{ref}} = 20\log_{10} \left| \frac{VSWR+1}{VSWR-1} \right| = -20\log_{10}|\Gamma| \ \ (dB) \tag{2.20}$$

2.4.9 Polarization

Polarization is defined as the orientation of the electric field of an electromagnetic wave. Polarization is in general described by an ellipse [1]. Two special cases of elliptical polarization are linear polarization and circular polarization as shown in figure 2.10. The initial polarization of a radio wave is determined by the antenna. With linear polarization the electric field vector stays in the same plane all the time. Vertically polarized radiation is somewhat less affected by reflections over the transmission path. Omnidirectional antennas always have vertical polarization. With horizontal polarization, such reflections cause variations in received signal strength. Horizontal antennas are less likely to pick up man-made interference, which ordinarily is vertically polarized. In circular polarization the electric field vector appears to be rotating with circular motion about the direction of propagation, making one full turn for each RF cycle. This rotation may be right hand or left hand. Choice of polarization is one of the design choices available to the RF system designer.
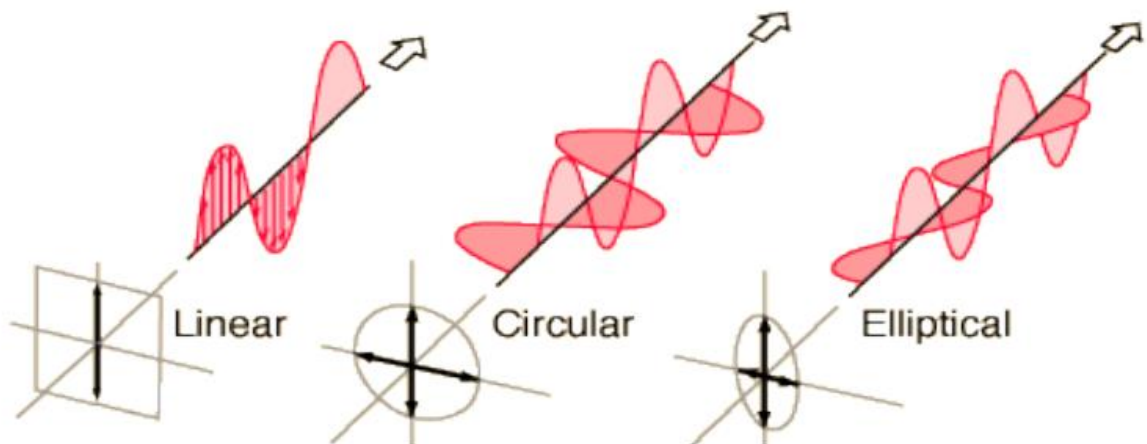

Figure 2.10: Electromagnetic wave Polarization classification [2].

2.5 Types of Antennas

There are several types of antennas which were developed since the past times due nowadays. In this section, a brief discussion of the different antennas according to their physical structures will be presented. The following types of antennas are: Wire antennas; aperture antennas, microstrip antennas, array Antennas, reflector antennas, and lens antennas [1].

2.5.1 Wire Antennas

Wire antennas are very simple and cheap, with linear or curved forms. such as dipoles, monopoles, loops, helices, Yagi–Uda and log-periodic antennas [1] as shown in figure 2.11.

• Dipoles are the simple one and most widely used types of antenna. A dipole can take several structures like open-end, two-wire transmission line. A typical structure of a dipole consists of two metal wires which are normally of equal length.

• The monopole antenna is half of the dipole antenna.

• Loop antennas can be a circular, square, triangle, rectangular or elliptical form.

• Helical antennas: with a shape defined by helices, similarly to a spring shape. Those antennas are used for space telemetry.
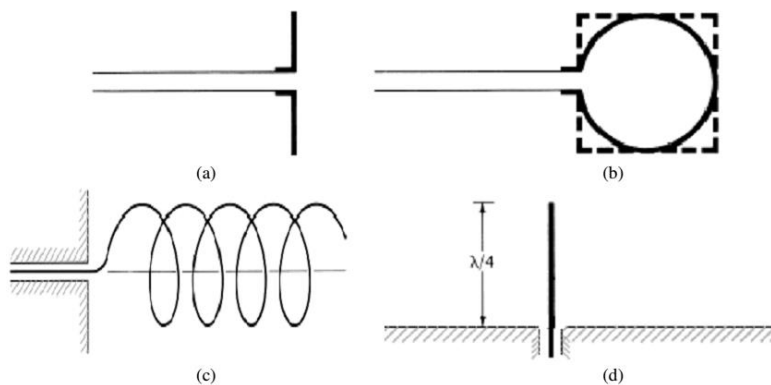

Figure 2.11: wire antenna types (a) Dipole (b) Loop (c) Helix (d) Monopole.

• Yagi–Uda Antenna: is popular type of end-fire antenna widely used in the VHF and UHF bands (30 MHz to 3 GHz) because of its simplicity, low cost and relatively high gain. The most noticeable application is for home TV reception and these can be found on the rooftops of houses. As shown in Figure 2.12.

20
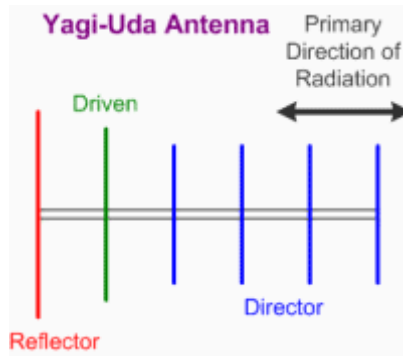
Figure 2.12: Yagi–Uda antenna.

• Log-Periodic Antennas: Similar to Yagi–Uda antenna as shown in figure 2.13. It produces a similar end-fire radiation pattern and directivity (typically between 7 and 15 dB more than isotropic radiator) to the Yagi–Uda and, is widely used in the VHF and UHF bands. However, Yagi–Uda antennas have wider bandwidth and each element is connected to the source and can be seen as a feeder [1].
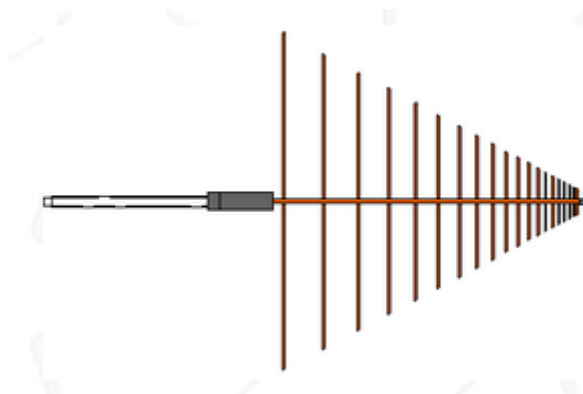
Figure 2.13: Log-Periodic antenna.

2.5.2 Aperture Antennas

There are many different geometrical configurations of an aperture antenna. They may take the form of a waveguide or a horn whose aperture may be square, rectangular, circular, elliptical, or any other configuration see figure 2.14. Aperture antennas are very practical for space applications, because they can be flush mounted on the surface of the spacecraft or aircraft. Horn antennas are the simplest and one of the most widely used forms of microwave antenna.
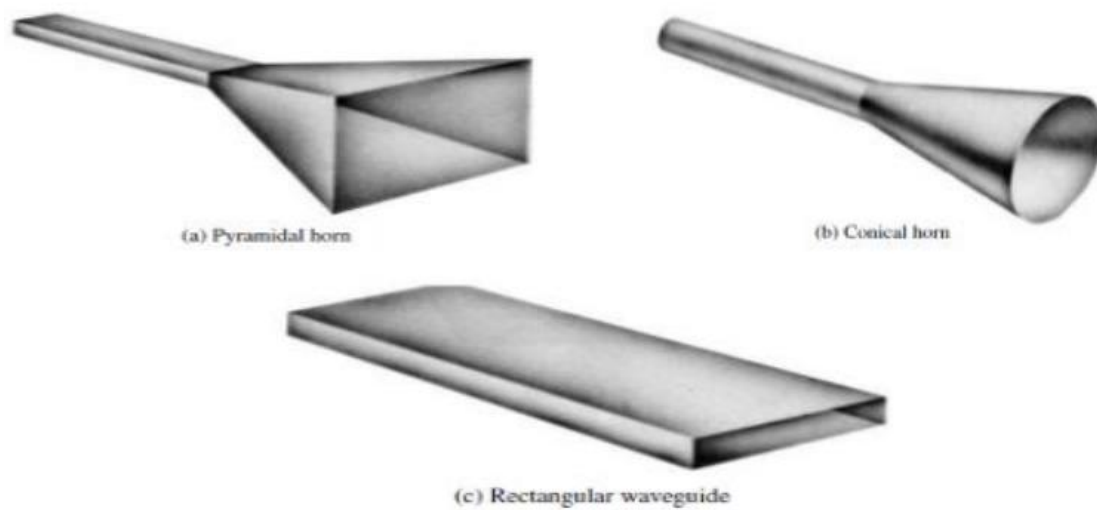
Figure 2.14: Aperture antenna shapes [3].

2.5.3 Array Antennas

A lot of applications require radiation characteristics that may not be achievable by a single element, so an antenna array could be a good solution. The arrangement of the array may be such that the radiation from the elements adds up to give a radiation maximum in a particular direction, minimum in others, or otherwise as desired. Different array configurations are shown in figure 2.15. The major advantages of an array are: the flexibility to form a desired radiation pattern, the high directivity and gain [1].
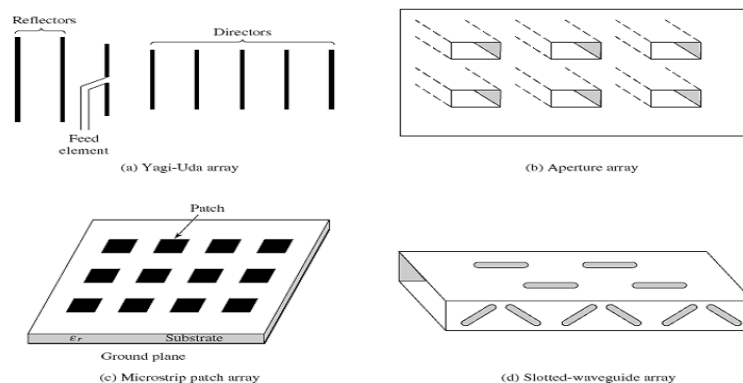
Figure 2.15: wire, aperture, and microstrip array configurations [1].

2.5.4 Reflector Antennas

Reflector antennas, also known as satellite dish antennas, are a specific type of antennas for long distance communications. They are probably the most widely used antennas for high-frequency and high-gain applications in radio astronomy, radar, microwave and millimeter wave communications and satellite tracking and communications see figure 2.16 [1].
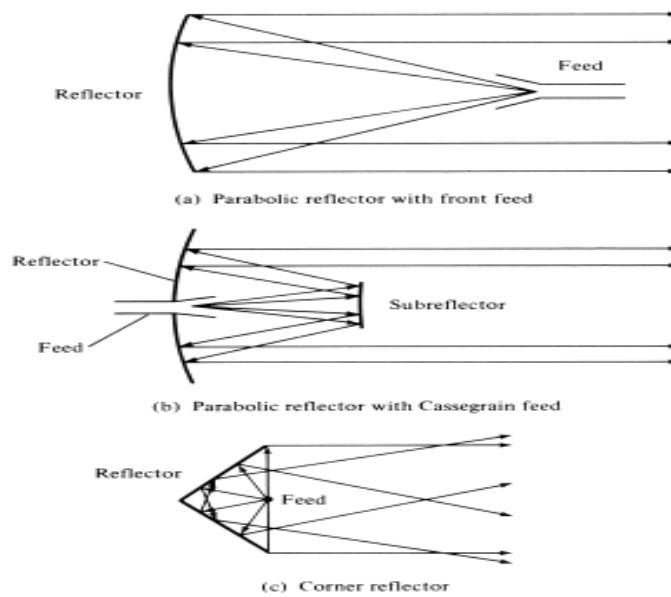
Figure 2.16: Lens antenna types [3].

2.5.5 Lens Antennas

Lens antennas can transform various forms of divergent energy into plane waves. They are suitable for high-frequency more than 4 GHz applications. There are many types as shown in figure 2.17, but the most important two types are delay lenses, in which the electrical path length is increased by the lens medium (using low-loss dielectrics with a relative permittivity greater than one, such as Lucite or polystyrene), and fast lenses, in which the electrical path length is decreased by the lens medium (using metallic or artificial dielectrics with a relative permittivity smaller than one) [1].
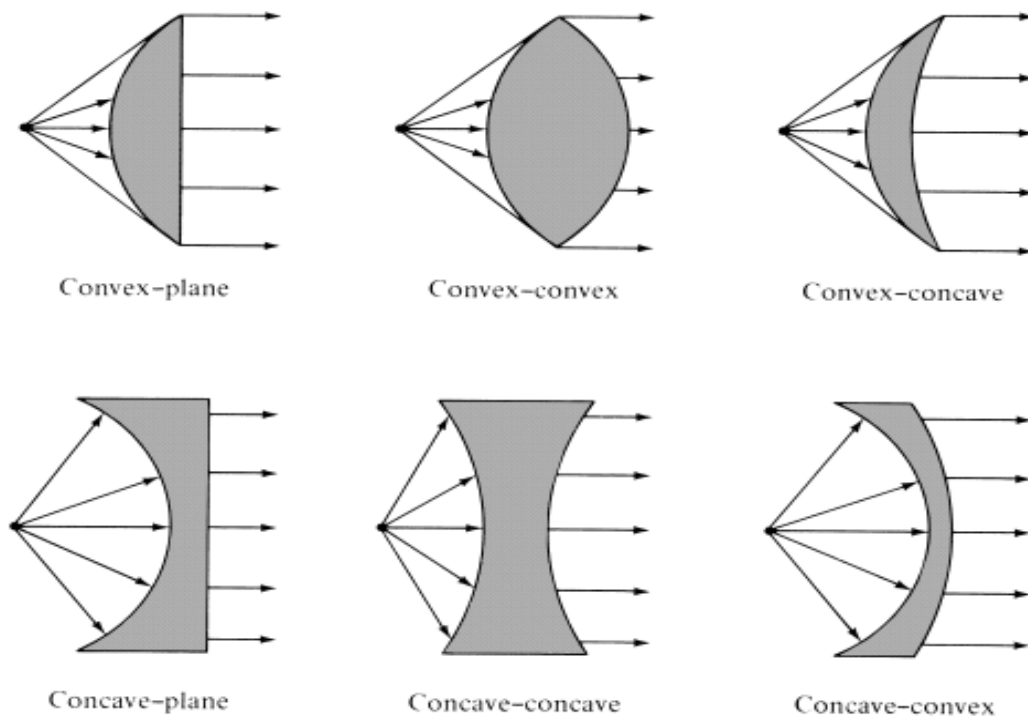
Figure 2.17: Lens antenna shapes [3].

2.6 Microstrip Patch Antenna and Design Procedure

The idea of microstrip antenna was first proposed by Deschamps in 1953 [4] and a patent in 1955. However, the first antenna was developed and fabricated during the 1970's when good substrates became available [4, 5]. Microstrip antenna is also referred as a patch antenna. Microstrip patch antenna consists of a radiating patch on one side of a dielectric substrate and a ground plane on the other side as shown in Figure 2.18. The patch is generally made of a conducting material such as copper or gold and can take any possible shape.
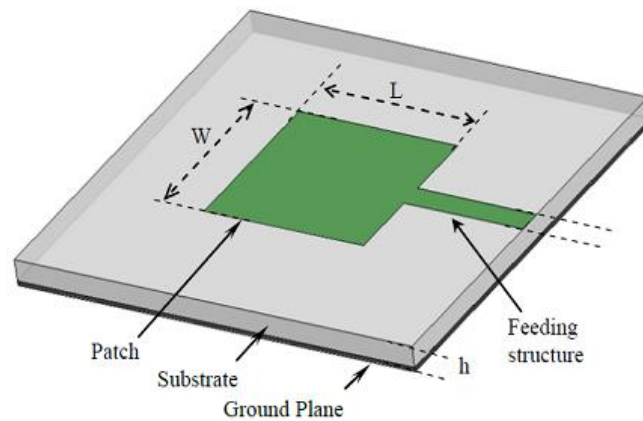
Figure 2.18: Basic microstrip patch antenna [5]

There are several shapes that can be used as the radiating patch. The radiating patch may be square, rectangular, thin strip (dipole), circular, elliptical, triangular, combination of these shapes or any other configuration [5]. Every shape has its own characteristics but square, rectangular, and circular are the most common configurations because of their easier analysis and fabrication.

2.6.1 Advantages and Disadvantages of Microstrip Antennas

The microstrip patch antenna has several advantages that proved to be an excellent radiator for many applications. But it also has some disadvantages. Even though the microstrip patch antenna suffers several disadvantages its many advantages have made it suitable to be used in wireless applications.

2.6.1.1 Advantages

i) They are lightweight, low volume and thin profile configuration. These make them to be easily incorporated into any package

ii) Low profile planar configuration that can be easily made conformal to host surface; which fits the shape design and needs of modern communication equipment.

iii) They can be made compact for use in personal mobile communication.

iv) The microstrip antenna shape flexibility enables mounting them on a rigid surface which makes them mechanically robust.

25

v) Using printed-circuit technology leads to a low fabrication cost hence can be manufactured in large quantities

vi) Supports both linear polarization and circular polarization.

vii) They accept for dual and triple frequency operations.

viii) They Can be easily integrated with microwave integrated circuits (MICs) on the same substrate.

2.6.1.2 Disadvantages:

i) Narrow bandwidth;

ii) They can only be used in low power applications and low power handling capability.

iii) Relatively poor radiation efficiency - radiate only in half-space.

iv) High losses resulting from surface wave excitation, conductor and dielectric losses.

2.6.2 Feeding Techniques

The following feeding techniques are used for patch antennas,

• Microstrip transmission-line feed

• Aperture coupling feed

• Coaxial probe feed

• Proximity coupling feed

These methods can be contacting or non-contacting. Contacting methods involve direct contact between the transmission line and the radiating surface. The non-contacting methods use electromagnetic field coupling to transfer the power to the patch [1].

2.6.2.1 Microstrip Transmission-Line Feed

A microstrip feed line is a strip that is much narrower than the patch. This feed is very easy to fabricate and easily matched by controlling the inset position [8]. The feed is connected to one side of the patch as shown in Figure 2.19. The transmission-line and the patch are made from the same material.
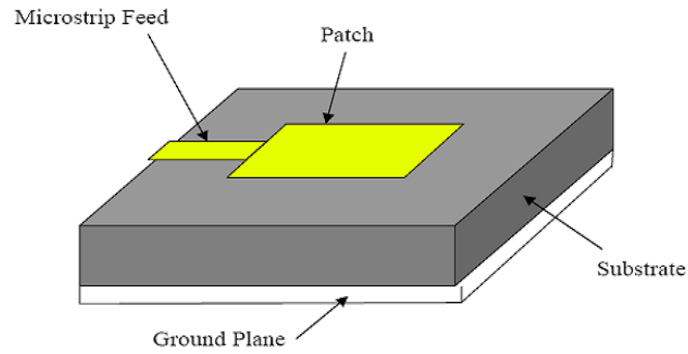
Figure 2.19: Patch with feed line [9]

2.6.2.2 Aperture Coupling Feed

Aperture coupling is more difficult to fabricate and leads to narrow band-width. The geometry consists of two substrates separated by a ground plane. The bottom side of the substrate is fed by a transmission-line and the energy is coupled to the patch through a slot as depicted in Figure 2.20 [8].

The substrate on top has a low dielectric constant while the bottom substrate is a higher material with a non-contacting feed. By controlling the length of the slot or the width of the transmission-line, matching is performed.
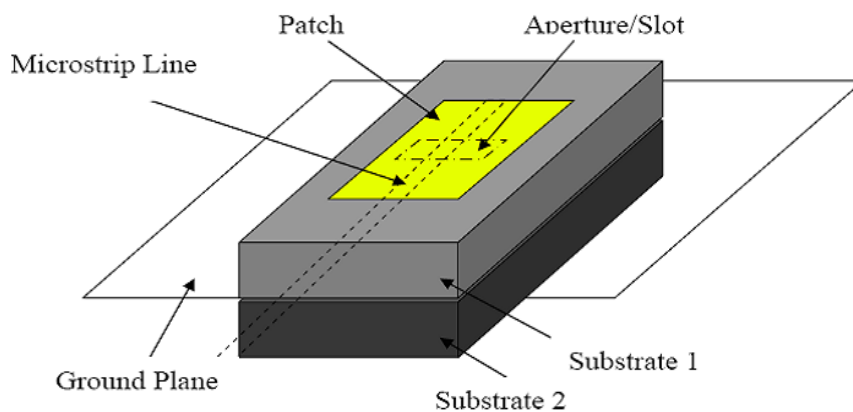
Figure 2.20: Aperture-coupled feed [9]

2.6.2.3 Coaxial Probe Feed

The coaxial probe feed has a narrow bandwidth. It consists of two conductors. The outer conductor is connected with the ground plane while the inner conductor is connected to the radiating patch as shown in Figure 2.21 [9]. Coaxial probe feed is easy to fabricate and match. It is very difficult to model for thick substrates; the coaxial feed introduces an inductance into the feed that may need to be taken into account. the probe will also radiate, which can lead to radiation in undesirable directions.
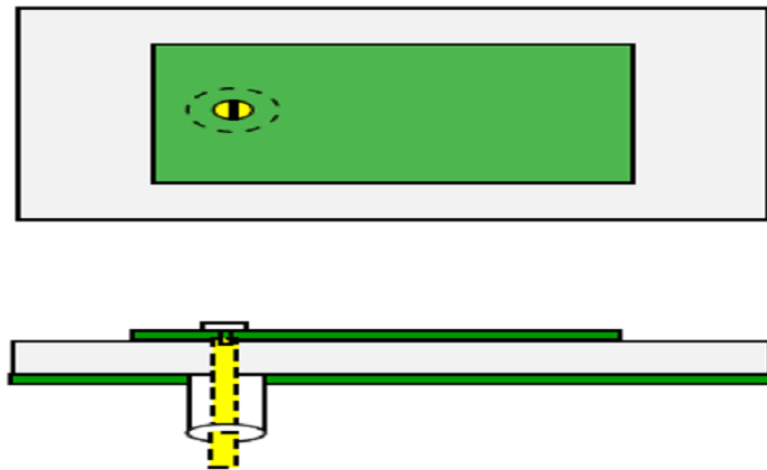
Figure 2.21: Top and side view of coaxial feeding

2.6.2.4 Proximity Coupling Feed

In proximity coupling, the microstrip line is placed between two substrates as shown in Figure 2.22 [9]. The upper substrate has a radiating patch on top. It is easy to model but difficult to fabricate. The bandwidth of the proximity coupling feed is very large. This coupling is capacitive and has low spurious radiation.
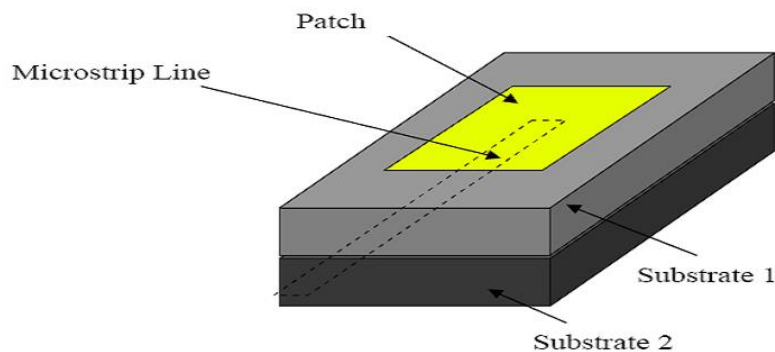
Figure 2.22: Proximity-coupled Feed

28

2.7 Transmission Line Model Analysis

The patch and ground-plane are separated by a dielectric. The patch conductor is normally copper. The patches are usually photo etched on the dielectric substrate. The substrate is usually non-magnetic. The relative permittivity of the substrate is normally in the region between 1 and 4, which enhances the fringing fields [3]. The rectangular patch is characterized by its length L, width w and thickness h, as shown in Figure 2.23 below.
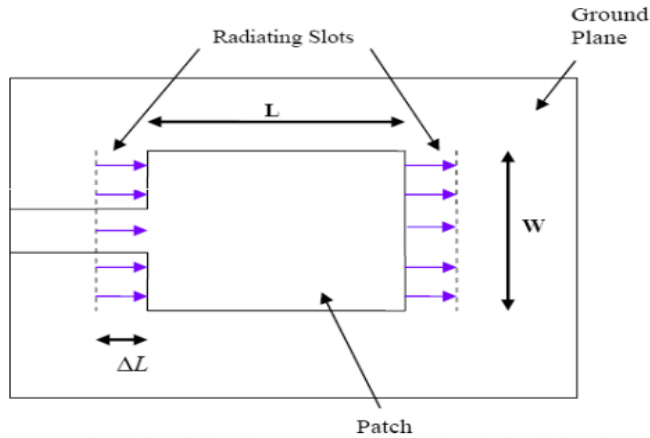
Figure 2.23: a rectangular microstrip patch antenna with fringing fields

An effective dielectric constant (ε_{reff}) must be obtained in order to account for the fringing and the wave propagation in the line. The value of, ε_{reff} is slightly less than ε_r because the fringing fields around the periphery of the patch are not confined in the dielectric substrate but are also spread in the air. It can be expressed by [1]:

$$\varepsilon_{\text{reff}} = \frac{\varepsilon_r + 1}{2} + \frac{\varepsilon_r - 1}{2}\left(1 + 12\frac{h}{w}\right)^{\frac{1}{2}}, \qquad (2.21)$$

where

ε_{reff} = Effective dielectric constant

ε_r = Dielectric constant of substrate

h = Height of dielectric substrate

W = Width of patch

For a given resonance frequency f_o, the effective length is given by [1]:

$$L_{\text{eff}} = \frac{c}{2f_o\sqrt{\varepsilon_{\text{reff}}}} \qquad (2.22)$$

The fringing fields along the width can be modeled as radiating slots and electrically the patch of the microstrip antenna looks greater than its physical dimensions. The dimensions of the patch along its length have now been extended on each end by a distance, ΔL.

The ΔL can be expressed as [1]:

$$\Delta L = 0.412h\left(\frac{(\varepsilon_{reff}+0.3)}{(\varepsilon_{reff}-0.258)}\left[\frac{\frac{w}{h}+0.264}{\frac{w}{h}+0.8}\right]\right) \tag{2.23}$$

The effective length of the patch L_{reff} now becomes:

$$L_{eff} = L + 2\,\Delta L\,, \tag{2.24}$$

where

ΔL = Length due to fringing effects

L = Length of patch

L_{eff}= Effective length of the patch

h = Height of dielectric substrate

W = Width of patch

For efficient radiation the width, W is given by [1]:

$$W = \frac{c}{2f_o\sqrt{\frac{\varepsilon_r+1}{2}}} \tag{2.25}$$

References

[1] C. A. Balanis, Antenna Theory, Analysis and Design, 3rd edition, John Wiley & Sons, Inc., 2005.

[2] C.Rohner, Antenna basics, Rohde & Schwarz, http://www.rohde-schwarz.com/.

[3] J. R. Jame, P. S Hall and C. Wood "Microstrip Antenna Theory and Design ". London, United Kingdom Peter Peregrinus Ltd.67-71. 2006.

[4] Kumar, Girish and Ray.K.P. "Broadband Microstrip Antennas" Artech House,2003.

[5] Kin- Lu Wong, "Compact and Broadband Microstrip Antennas" John Wiley & Sons, Inc., 2002.

[6] Y.Huang, Antennas from Theory to Practice, first edition, Wiley, Oct.2008.

[7] W. L. Stutzman, G. A. Thiele, "Antenna Fundamentals and Definitions," in Antenna theory and design, PP. 1-52, 2nd ed., New York: Wiley, 1998.

[8] J. Yang; Chen Wu; Litva, J. "Microstrip Ring Antennas for PCS Application" Publication Year: 1996, Page(s): 1594 - 1597 vol.3

[9] S K Behera, "Novel Tuned Rectangular Patch Antenna As a Load for Phase Power Combining" Ph.D Thesis, Jadavpur University, Kolkata.

[10] D.M. Pozar, Microwave Engineering, Third Edition, John Wiley & Sons, 2005, Inc. ISBN 0-471-44878-8.

[11] P. Dhande "Antennas and its Applications," DRDO Science Spectrum, pp.66-78, 2009.

[12] C. A. Balanis, Modern Antenna Handbook, first edition, Wiley, 2008.

[13] L.Meyer, "Calculating Antenna System Return Loss as Viewed through the RF Path.", Whitepaper, Andrew Communication Scope, TP-102660-EN, http://www.andrew.com, December 2009.

[14] D.M. Pozar, Microwave Engineering, Third Edition, John Wiley & Sons, 2005, Inc. ISBN 0-471-44878-8.

3

Rectifier Circuits

3.1 Introduction

The rectifier circuit is a circuit which rectifies AC voltage into DC voltage. In other words, rectifier is an electrical device composed of one or more diodes that converts alternating current (AC) to direct current (DC) as shown in figure 3.1. A diode is like a one-way valve that allows an electrical current to flow in only one direction. This process is called rectification [1].

Rectification produces a type of DC that encompasses active voltages and currents, which are then adjusted into a type of constant voltage DC, although this varies depending on the current's end-use. The current is allowed to flow uninterrupted in one direction, and no current is allowed to flow in the opposite direction [2].

A rectifier can take the shape of several different physical forms such as solid-state diodes, vacuum tube diodes, mercury arc valves, silicon-controlled rectifiers and various other silicon-based semiconductor switches.

Figure 3.1: rectifier [3]

3.2 Rectifier

The simplest design that can be used is a peak detector or half wave peak rectifier. This circuit requires only a capacitor and a diode to function. The schematic is shown in Figure 3.2. The AC wave has two halves, one positive and one negative. On the positive half, the diode turns on and current flows, charging the capacitor. On the negative half of the wave, the diode is off such that no current is flowing in either direction. Now, the capacitor has voltage built up which is equal to the peak of the AC signal, hence the name. Without the load on the circuit, the voltage would hold indefinitely on the capacitor and look like a DC signal, assuming ideal components. With the load, however, the output voltage decreases during the negative cycle of the AC input, shown in Figure 3.3.
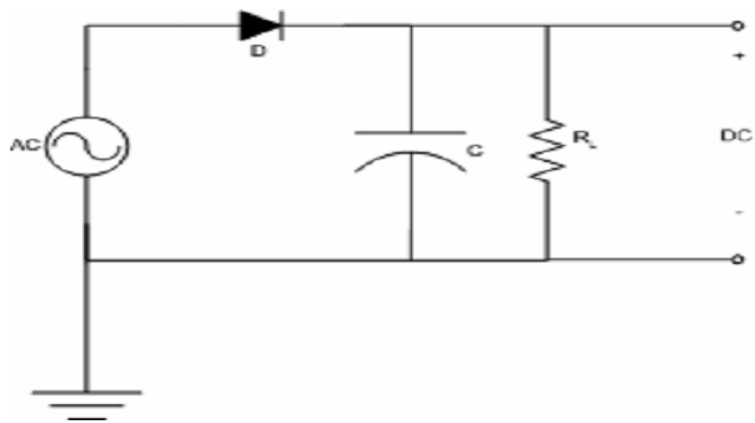
Figure 3.2: Peak Detector
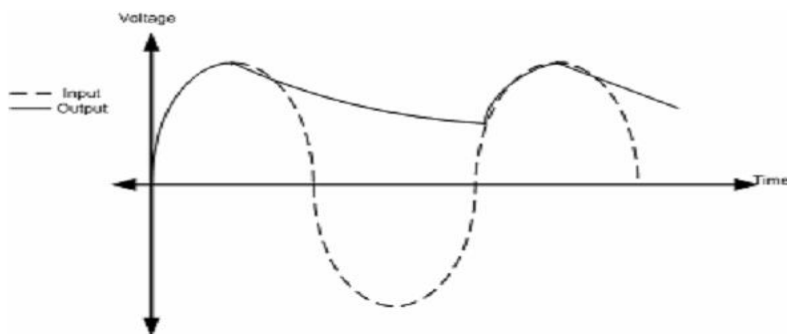
Figure 3.3: Half-wave Peak Rectifier Output Waveform

The voltage decreases in relation to the inverse of the resistance of the load, R, multiplied by the capacitance C. This circuit produces a lot of ripple, or noise, on the output DC of the signal. With more circuitry, that ripple can be reduced.

The full-wave rectifier circuit is shown in Figure 3.4. where in the positive half cycle, D1 is on, D2 is off and charge is stored on the capacitor and during the negative half, the diodes are reversed, D2 is on and D1 is off. The capacitor doesn't discharge, so the output has much less noise, as shown in Figure 3.5. It produces a cleaner DC signal than the half-wave rectifier, but the circuit itself is much more complicated with the introduction of a transformer.

Figure 3.4: Full-wave Rectifier [3]

Figure 3.5: Full-wave Rectifier Output Waveform [3]

3.3 Schottky Diode Fundamentals

Schottky diodes are constructed of a metal-to-N junction rather than a P-N semiconductor junction. Also known as hot-carrier diodes, Schottky diodes are characterized by fast switching times (low reverse-recovery t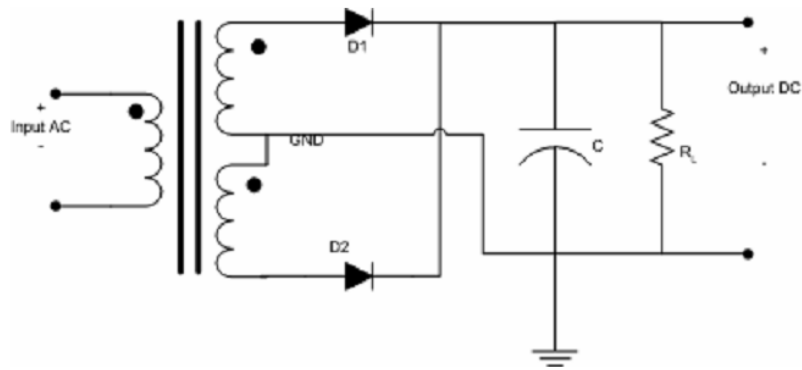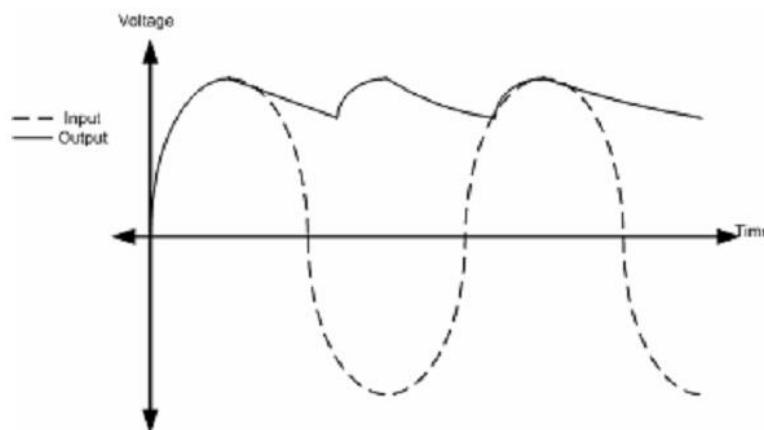ime), low forward voltage drop (typically 0.25 to 0.4 volts for a metal-silicon junction), and low junction capacitance [4].

The Schottky diode is the principal element of a wireless energy harvesting device, therefore it is important to provide a correct model. Zero-bias diodes are necessary because they have relatively low barrier (high saturation current), which compared to externally biased detector diodes, results in a higher output voltage for low power input levels. The equivalent electrical circuit of a Schottky diode is shown Figure 3.6.
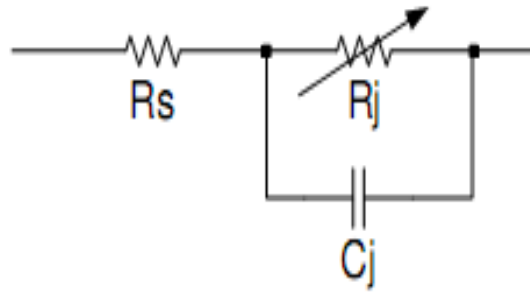
Figure 3.6: Equivalent circuit of a Schottky diode [12].

with C_j the junction capacitance (diode voltage dependent) (in Farad), R_s the bulk series resistance (in Ω) and R_j the junction resistance of the diode (in Ω).

In order to obtain the maximum output, all the incoming RF voltage should ideally appear across R_j with no losses over R_s, so for low-power applications we are interested to choose a diode with the smallest series resistance value. The intrinsic diode is modeled as a varistor element that obeys the i-v law, as described in [8]:

$$i = I_s \left[\exp\left(\frac{1}{n} \Lambda_v \right) - 1 \right] \tag{3.1}$$

where I_s is the diode's saturation current and $\Lambda = \frac{q}{kT}$ is the reciprocal of the thermal voltage, q is the electronic charge, k is Boltzmann's constant, T is the physical temperature in Kelvins, and n is the diode ideality factor (emission coefficient).

Therefore, the saturation current I_s is given by:

$$I_s(T) = I_s(T_0)(\frac{T}{T_0})^{2/n}\exp[-\frac{q\psi_{ms}}{k}(\frac{1}{T} - \frac{1}{T_0})] \tag{3.2}$$

where T_0 is a reference temperature. The quantity ψ_{ms} is the metal-semiconductor Schottky barrier height (energy gap) at T_0 (e.g., 0.85 eV for A1 on GaAs).

The Schottky diodes has two main classes. The first class is the n-type silicon with a high-barrier and low values of series resistance The second class is the p-type silicon characterized by low barrier and high R_s For wireless energy harvesting applications, we are interested to use the second class (p-type diode). Although we have a high series resistance, the higher saturation current of the p-type diode results in a higher output voltage at low power levels compared to a n-type (100 times) [9].

In Figure 3.7, the simulated output voltage for two commercial Schottky diodes is presented: HSMS-285X (p-type) and HSMS-8205 (n-type). The diodes are loaded by a 1kΩ load resistor.
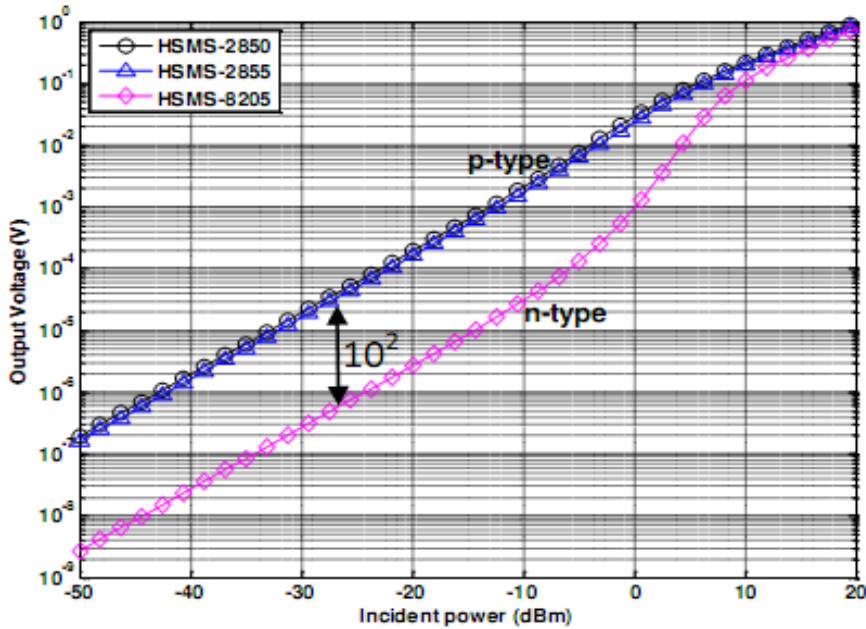

Figure 3.7: output voltage as a function of available input power for three commercially available Schottky diodes: Avago HSMS-285X (p-type) and HSMS-8205 (n-type). Diode loaded by a 1kΩ load [8].

In Figure 3.7, different voltage profiles can be observed between high and low power levels. we can also notice that for low incident power applications, e.g., wireless energy harvesting, the p-type Schottky diode is recommended since it provides a higher output voltage when compared to the n-type (10^2x).

From (3.1), the value of R_j of the diode decreases due to the value of circulating current I_b, i.e., the diode impedance being dependent of the RF input power. The junction capacitance has a large impact ahead the output voltage at high frequencies and when the series resistance has high values. The impact of the series resistance on the output DC voltage has been described in [9]. A simple multiplier parameter for the output voltage has been defined (3.3) related to the 3 components of the equivalent electrical circuit of a Schottky diode (Figure 3.6). If the series resistance increases the output voltage is strongly reduced by the multiplier M.

$$M=\frac{1}{1+\omega^2 C_j^2 R_s R_j} \tag{3.3}$$

where ω is the angular frequency (in rd/s)

The output voltage will be the primary goal of the harvester design. Nevertheless, the RF-DC conversion efficiency describes how powerful the rectifier is. A compromise should be obtained between a high-efficiency value and a specific output voltage required for a RF energy harvester.

In Figure 3.8, two typical harvester configurations are presented, a single diode and a voltage doubler. Obviously the voltage doubler provides a higher output than the single diode; however the RF-DC conversion efficiency is lower, as widely demonstrated in the literature [10]-[11]. The doubler puts the Schottky diodes in parallel with respect to the input RF signal, thus lowering the input impedance and reducing the complexity of the impedance matching network.
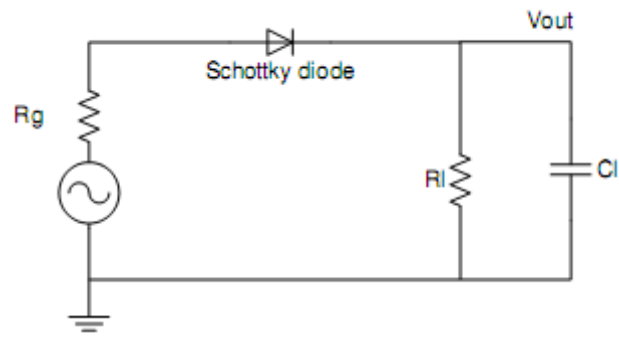
(a)
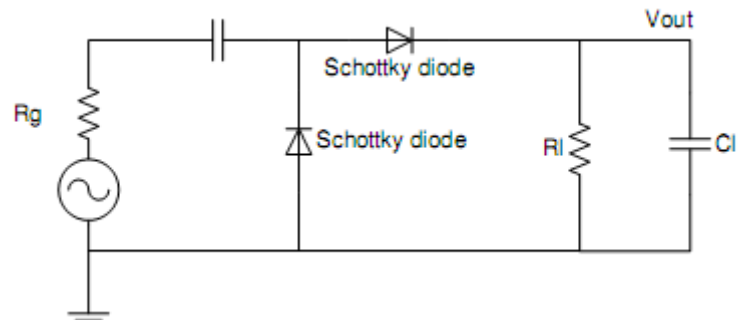
(b)

Figure 3.8: Harvester configurations: (a) single diode, (b) voltage doubler/double diode.

Figure 3.9: effect of number of stages on the efficiency of energy harvesting Circuit (with HSMS-2852 diodes) [11].

As shown in Figure 3.9, a single diode converter reaches only 45% of efficiency but it is for the smallest RF power (around -15dBm). This low input power is the main constraint for a wireless energy harvesting converter.

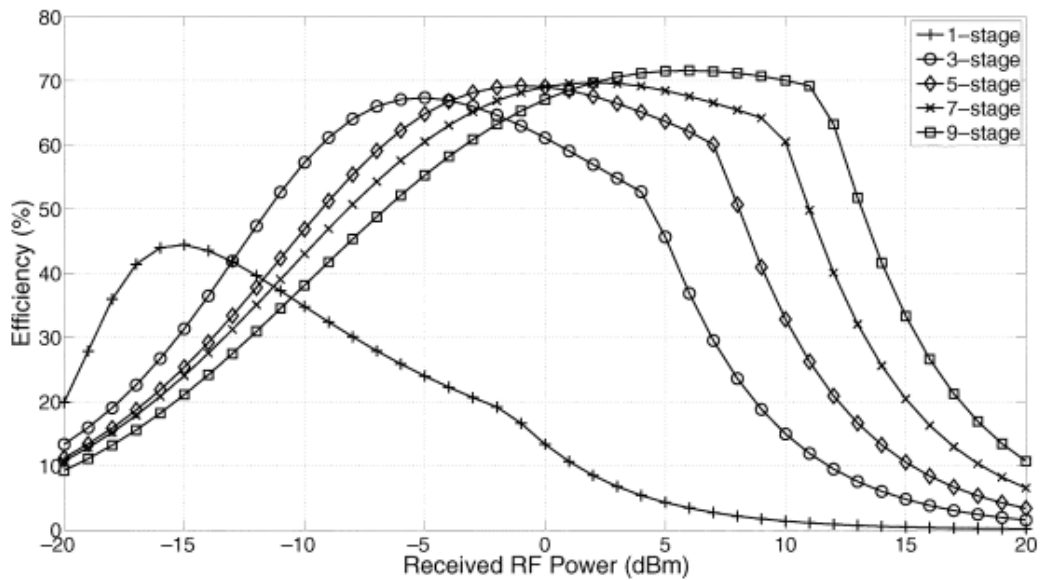As described before, the diode junction type can be determinant on a wireless energy harvesting device, the HSMS-285X (2850 and 2855) is p-type silicon and the HSMS-8205 is a n-type silicon. For low incident power an important difference on the output voltage can be noticed between both silicon types; the p-type diode presents a higher output voltage for low incident power, when compared to the n-type diode. Moreover, with a single diode, a high efficiency can be reached for low RF input power.

3.4 Design of the rectifier using Schottky diode

Villard voltage doubler circuit is designed and simulated by Advanced Design System (ADS) software. This circuit is optimized and achieved by using Schottky diode pair HSMS-285X for Rs= 25 Ω, Cj= 0.18 pF, Bv= 3.8 V which is chosen for applications below than 1.5 GHz. Table-3.1 shows the parameters value in the design [12] and for more detail on the used schottky diode family see (Appendix. A).

Table (3.1): HSMS285x Schottky Diodes spice parameter

Parameters	Units	HSMS-285X
Bv	V	3.8
C_{Jo}	pF	0.18
E_G	eV	0.69
I_{Bv}	A	3 E -4
I_s	A	3 E -6
N		1.06
R_s	Ω	25
$P_B(V_J)$	V	0.35
$P_T(XTI)$		2
M		0.5

The attractive features of this diode include: low forward voltage, low substrate leakage, fast switching and uses the non-symmetric properties of a diode to allow unidirectional flow of current under ideal situation. The equivalent linear model can be used for the diode is shown in Figure 3.6. Rs is series resistance of the diode, Cj is the junction capacitance and Rj is the junction [13].

The parameter extractions are given in Equation. (3.4)- (3.9).

$$Y_Z = Y_{Cj} + Y_{Rj} \tag{3.4}$$

Equation (3.4) related to the frequency of operation is given by:

$$Y_Z = jwc_j + \frac{1}{R_j} = \frac{jwc_jR_j + 1}{R_j} \tag{3.5}$$

The total impedance Z_T is given by:

$$Z_{T=}R_{s+} \frac{R_j}{jwc_jR_j + 1}, \tag{3.6}$$

where R_s and C_j are constants and the frequency of operation (w) is the only variable parameter. As the frequency increases, the value of Z is almost negligible compared to the series resistance R_S of the diode. From this, it can be concluded that the function of the diode is independent of the frequency of operation.

R_s is the series resistance of the circuit and junction resistance R_j is given by Equation. (3.7) [12].

$$R_j = \frac{8.33 * 10^{-5} * N * T}{I_b + I_s} \tag{3.7}$$

where

I_b = externally applied bias current in amps

I_S = saturation current

T = temperature, °K

N = ideality factor

3.5 Single Stage Voltage Multiplier

A single stage voltage multiplier circuit as shown in figure 3.10 also called as a voltage doubler because in theory, the voltage that is arrived on the output is approximately twice that at the input. The circuit consists of two sections; each comprises a diode and a capacitor for rectification. The RF input signal is rectified in the positive half of the input cycle, followed by the negative half of the input cycle. But, the voltage stored on the input capacitor during one half cycle is transferred to the output capacitor during the next half cycle of the input signal. Thus, the voltage on output capacitor is roughly two times the peak voltage of the RF source minus the turn-on voltage of the diode.
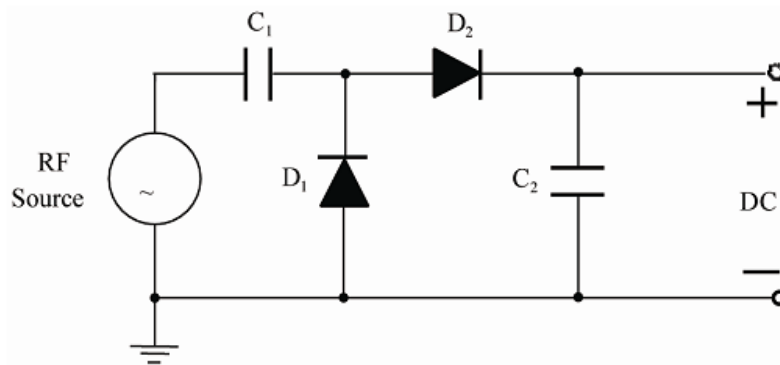

Figure 3.10: Single stage voltage multiplier circuit [14].

The most interesting feature of this circuit is that when these stages are connected in series. This method behaves akin to the principle of stacking batteries in series to get more voltage at the output. The output of the first stage is not exactly pure DC voltage and it is basically an AC signal with a DC offset voltage. This is equivalent to a DC signal superimposed by ripple content. Due to this distinctive feature, succeeding stages in the circuit can get more voltage than the preceding stages. If a second stage is added on top of the first multiplier circuit, the only waveform that the second stage receives is the noise of the first stage. This noise is then doubled and added to the DC voltage of the first stage. Therefore, the more stages that are added, theoretically, more voltage will come from the system regardless of the input. Each independent stage with its dedicated voltage doubler circuit can be seen as a single battery with open circuit output voltage V_{out}, internal resistance R_O with load resistance R_L, the output voltage, V_{out} is expressed as in Equation (3.9)[14].

$$V_{out} = \frac{V_0}{R_L + R_0} R_L \tag{3.8}$$

when n number of these circuits are put in series and connected to a load of R_L in Equation (3.8) the output voltage V_{out} obtained is given by this change in RC value will make the time constant longer which in turn retains the multiplication effect of two in this design of seven stage voltage doubler.

$$V_{out} = \frac{nV_0}{nR_L + R_0} R_L = V_0 \frac{1}{\frac{R_0}{R_L} + \frac{1}{n}} \tag{3.9}$$

The number of stages in the system has the greatest effect on the DC output voltage, as shown from Equations (3.8) and (3.9).

3.6 Seven Stage Voltage Multiplier

The seven stage voltage multiplier circuit design implemented in this thesis is shown in Figure 3.11. From the left side, there is a RF signal source for the circuit followed by the first stage of the voltage multiplier circuit. Each stage is stacked onto the previous stage as shown in the Figure 3.11. Stacking was done from left to right for simplicity instead of conventional stacking from bottom to top.
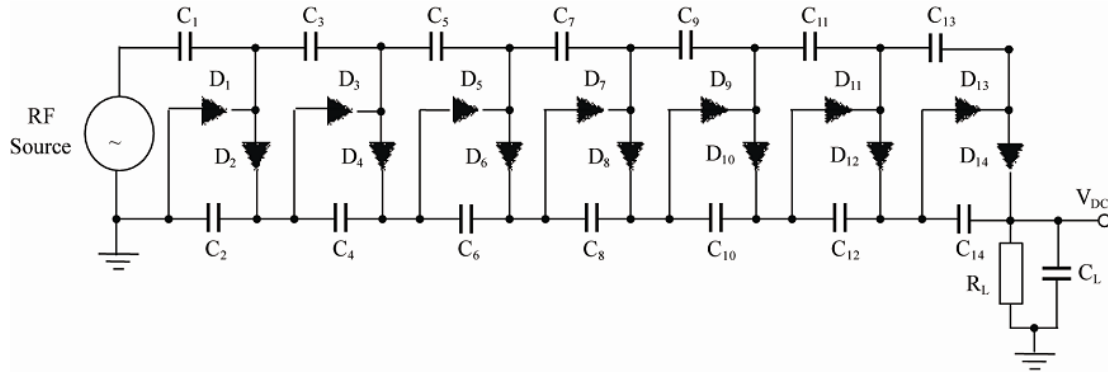
Figure 3.11: Schematic of 7 stage voltage multiplier.

The circuit uses eight zero bias Schottky surface-mount Agilent HSMS-285X series, HSMS-2850 diodes. The special features of these diode is that, it provides a low forward voltage, low substrate leakage and uses the non-symmetric properties of a diode that allows unidirectional flow of current under ideal conditions. The diodes are fixed and are not subject of optimization or tuning. This type of multiplier produces a DC voltage which

depends on the incident RF voltage. Input to the circuit is a predefined RF source. The voltage conversion can be effective only if the input voltage is higher than the Schottky forward voltage.

The other components associated with the circuit are the stage capacitors. The chosen capacitors for this circuit are of through-hole type, which make it easier to modify for optimization, where in [15] the optimization was accomplished at the input impedance of the CMOS chip for a three stage voltage multiplier. The circuit design in this thesis uses a capacitor across the load to store and provide DC output voltage and its value only affects the speed of the transient response. Without a capacitor across the load, the output is not a good DC signal, but more of an offset AC signal.

In addition, an equivalent load resistor is connected at the final node. The output voltage across the load decreases during the negative half cycle of the AC input signal. The voltage decreases are inversely proportional to the product of resistance and capacitance across the load. Without the load resistor on the circuit, the voltage would be hold indefinitely on the capacitor and look like a DC signal, assuming ideal components. In the design, the individual components of the stages need not to be rated to withstand the entire output voltage. Each component only needs to be concerned with the relative voltage differences directly across its own terminals and of the components immediately adjacent to it. In this type of circuitry, the circuit does not change the output voltage but increases the possible output current by a factor of two. The number of stages in the system is directly proportional to the amount of voltage obtained and has the greatest effect on the output voltage as explained in the Equation (3.9).

Reference

[1]   M. H. Rashid, POWER ELECTRONICS HANDBOOK, 3rd edition, Prentice Hall,2011.

[2]   http://www.techopedia.com/definition/681/rectifier

[3]   http://www.efxkits.us/types-of-rectifiers-with-workings/

[4]   A. Reinders, "Options for Photovoltaic Solar Energy Systems in Portable Products," TMCE, 2002.

[5]   M. Veefkind and S. F. J. Flipsen, "Gathering data on the energy to be harvested with portable consumer products, method and equipment," in Proceedings of the ISES EuroSun Congress, 2004.

[6]   M. Veefkind, "Industrial design and PV-power, challenges and barrieres," in Proceedings of the ISES Solar World Congress, 2003.

[7]   ATA LABS. [Online] Available: http://atlalabs.com/

[8]   R. G. Harrison and X. Polozec, "Nonsquarelaw Behavior of Diode Detectors Analyzed by the Ritz Galerkin Method," Microwave Theory and Techniques, IEEE Transactions on, no. 5, pp. 840-846, 1994.

[9]   Avago technologies Corp. (2010, July). Designing the virtual battery. [Online]. Available:http://www.avagotech.com/docs/5966-0785E.

[10]   J. Essel, D. Brenk, J. Heidrich, R. Weigel, "A highly efficient UHF RFID frontend approach," Wireless Sensing, Local Positioning, and RFID, 2009. IMWS 2009. IEEE MTT-S International Microwave Workshop on , vol., no., pp.1-4, 24-25, Sept. 2009.

[11]   P. Nintanavongsa, U. Muncuk, D.R. Lewis, K.R. Chowdhury, "Design Optimization and Implementation for RF Energy Harvesting Circuits," Emerging and Selected Topics in Circuits and Systems, IEEE Journal on , vol.2, no.1, pp.24-33, Mar. 2012.

[12]   HSMS-2850, "Surface Mount Zero Bias Schottky Detector Diodes. http://www.crystal-radio.eu/hsms285xdata.pdf.

[13]   Lenin A. and Abarna P. 2014. Design and Simulation of Energy Harvesting System Using GSM Signal. International Journal of Latest Trends in Engineering and Technology. 3(4): 19-25

[14]   D. W. Harrist, "Wireless Battery Charging System Using Radio Frequency Energy Harvesting," M.S. Thesis, Uni- versity of Pittsburgh, Pittsburgh, 2004.

[15]   E. Bergeret, J. Gaubert, P. Pannie and J. M. Gaultierr, "Modeling and Design of CMOS UHF Voltage Multiplier for RFID in an EEPROM Compatible Process," IEEE Transactions on Circuits and Systems-I, Vol. 54, No. 10, 2007, pp. 833-837. doi:10.1109/TCSII.2007.902222

4

Design of Rectenna

4.1 Introduction

Rectifying antennas have become very popular over the past few years due to the increasing need for new ways to recycle energy. New advancements in antenna design, circuit design, and efficiency optimization have fueled the study of RF energy harvesting. We will introduce some studies on rectenna design and the advancements that have already taken place.

4.2 Literature review

In [1], a dual polarized patch rectenna array was developed; the rectenna consists of a coplanar strip-line (CPS) truncated patch antenna and CPS band-pass filter. The design compared single shunt diode rectifier with dual diodes rectifier. It was shown that the single shunt diode works as a half-wave rectifier and the output DC voltage of single shunt diode rectenna only half of that of dual diodes rectenna. The dual-diode rectenna achieved an RF to DC conversion efficiency of 76% at 5.8 GHz. In addition a rectenna array formed by the rectenna element was demonstrated and the investigation for various interconnection methods for a rectenna array was reported.

In [2], an RF energy harvesting circuit has been designed based on single-stage voltage multiplier rectifier which is capable to convert RF energy from any antenna operating at 2.45 GHz to dc power.

A 5 KΩ resistive load used to ensure the recycling of optimum dc power and the output dc power with respect to the input RF power varies from 9.2 μW to 359.5 μW respectively for the received RF power varying from -15 dBm to 0 dBm.

In [3], microstrip antenna array linearly polarized with high gain, operating at 915MHz for energy harvesting was designed. The optimization theory for wireless power

transmission efficiency has been used to design the feeding network of the antenna array to achieve the maximum power transmission efficiency with a given antenna configuration. A three-stage Dickson charge pump circuit rectifier with a light emitting diode (LED) as the resistive load connected to the antenna array terminal. For a given input power of 10dBm fed into a circularly polarized transmitting antenna with 6dBi gain, the maximum distance for lighting the LED is 51cm. and the best rectifier efficiency is 41% when the input power fed into the rectifier is 10dBm.

In [4], a high efficiency dual-frequency dipole rectenna operated at 2.45 and 5.8 GHz wireless power transmission was investigated. The rectenna consists of a receiving dual-frequency dipole antenna, a CPS input low-pass filter, two CPS band-pass filters, a rectifying diode and a microwave block capacitor. The measured conversion efficiencies achieved at free space are 84.4% and 82.7% at 2.45 GHz and 5.84 GHz, respectively.

In [5], a 900 MHz rectenna for wireless energy harvesting application was designed. It consists of a dipole antenna designed in a square shape connected to a highly efficient rectifier in a doubler voltage structure using HSMS 2862 Schottky diode and a matching network. Measuring an efficiency of 60% for 5 mW input power. The use of square shape increases the aperture efficiency and the gain of the antenna resulting in more power for the rectifier circuit and obtaining more dc power at the output of the circuit. The measured gain of the antenna was 1.8 dBi at 900 MHz. The rectifier circuit and the antenna were measured individually, and they were in good agreement with the simulation results. Then they were integrated together and fabricated on a single 5880 Rogers substrate and measured as a rectenna. The rectenna was able to harvest power from a 900 MHz wireless source, which produced about 80 mW/m2 located 1.2 m from the rectenna.

In [6], a novel rectenna design is presented for Wireless Power Transmission. The design would receive and convert microwave of 2.45GHz to DC. The proposed Rectenna consists of Microstrip patch antenna, zero biased Schottky diode HSMS 286b for rectification with Load resistance is varied from 100 Ω to 5 MΩ to find the optimum value for maximum voltage conversion and Low Pass filter is added between antenna and rectifier. Variation of 0.2 volt to 0.7 volt is observed between simulated and fabricated results.

The authors in [7] present a high efficiency 2.45-GHz rectenna that can harvest low input RF power effectively. a simple antenna structure with a high gain of 8.6dBi is proposed

47

to directly match the rectifying circuit at 2.45GHz and mismatch it at the second and third harmonics so that the use of band pass filter between the antenna and rectifying circuit can be eliminated. The rectenna shows a maximum conversion efficiency of 83% with a load resistance of 1400 Ohm. It is demonstrated that the overall efficiency of the proposed rectenna can achieve 80.3% and 50% with power density of 1.95 and 0.22µW/cm, respectively.

In [8], a circuit consists of microstrip patch antenna and Villard voltage doubler circuit which operates at 900 MHz band with a three stages of Schottky diode HSMS-285B voltage doubler circuit is designed, simulated and matched to the antenna design. The simulated result shows that the impedance bandwidth covers 0.82-0.93 GHz and the directivity of the main lobe is found to be 6.5 dBi at frequency of 0.9 GHz. The output voltage of the rectifier is 5.014 V which indicates the suitability for charging mobile applications.

In [9], RF energy harvesting system from the ambient surroundings radio frequency range of ISM band of 2.4GHz proposed. The main module of system is Microstrip antenna designed in the RF range of 2.2 - 3GHz with a partial Ground plane and 2 slots in the patch obtained the return loss of -22db and rectification occurs by rectifying the input RF signal by Voltage Multiplication Circuit. The output voltage obtained using 2 element Yagi Uda antenna is 750mV. While using the presented design here 2.4 GHz Microstrip antenna we could obtain the output voltage of 80mV.

IN [10], Deep Brain Stimulation (DBS) which is a treatment for neurogical and psychiatric disorder that works effectively is presented. Energy harvesting can be used to meet the needs of battery-less device for DBS application. The proposed antenna comes with the combination of the rectifying circuit. A coaxial line is used to feed the radiating patch with 50Ω. The designed antenna is chosen to be used for laboratory rat studies. Since the real head is much complex therefore experimental validation for a rat study is required before implementation. The antenna shows the good performance where the bandwidth is between 909-927 MHz which including the ISM band of 915 MHz with maximum antenna gain of 18.28 dB at free space.

The author in [11] proposed a multiband microstrip antenna with to collect the RF energy at the desired frequency including the ISM band. Multi resonator antenna is proposed to collect RF energy at multiple bands. High dielectric substrate, RogercRT/d6006 limits

the overall antenna dimensions. The antenna model exhibits the narrow width multiband. Furthermore, the analysis of the current flow across the surface of the antenna is performed. RF propagations, cellular base station and ISM communications was collected by the receiving multiband antenna.

In [12], the performance of the square slot antenna for wireless energy harvesting is presented. The slots cut on the top while the ground plane to improve the gain and return loss. Also the slots give bandwidth which limits the use of application but low profile high gain antenna can be easily configured. The antenna achieved to improve the return loss, keep the height of the substrate low and maintaining the directivity of the structure. The antenna use microstrip feed line and a substrate of Roger RT5880. The simulation result compares the gain and return loss without slots, with square slots on the patch and square slots on both the patch and the ground. It is shown that by introducing of the square slots, the return loss and gain has improved, and the resonant frequency shifted to 2.44 GHz. An improvement of the antenna performance always received a great intention.

4.3 Design of the Patch Antenna

The patch antenna has been simulated by CST microwave studio and the design is based on theoretical calculations from Chapter 2.

4.3.1 Microstrip Patch Antenna with Inset Feed

The designed microstrip patch antenna with inset feed has a full ground plane dimensions (WS x LS) $115 \times 140 mm^2$. The width of the patch (WP) is 91.7 mm and the length of the patch (LP) is 75 mm. The antenna is designed on a 1.6 mm thick FR-4 substrate ($\varepsilon_r = 4.3$). The 50-Ω line is about 3.1 mm wide as calculated by CST software. As seen from Figure 4.1 there is an Lf =32.3 mm long transmission line that is connected to the patch with feeding width Wf=3.1 mm. The inset of feed has a dimension of $3.12 \times 24.3 mm^2$. Figure 4.2 shows the S_{11} simulation of the patch antenna.
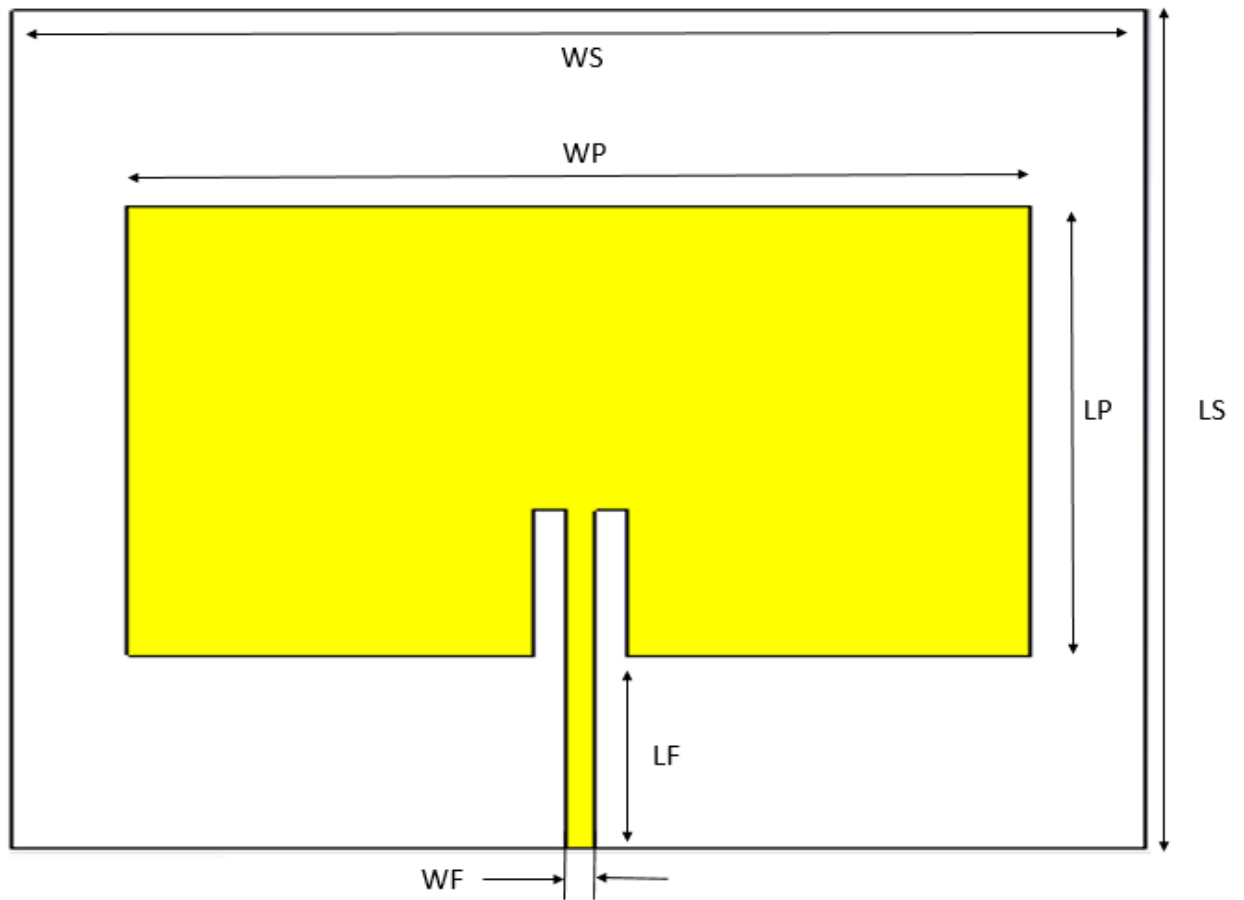
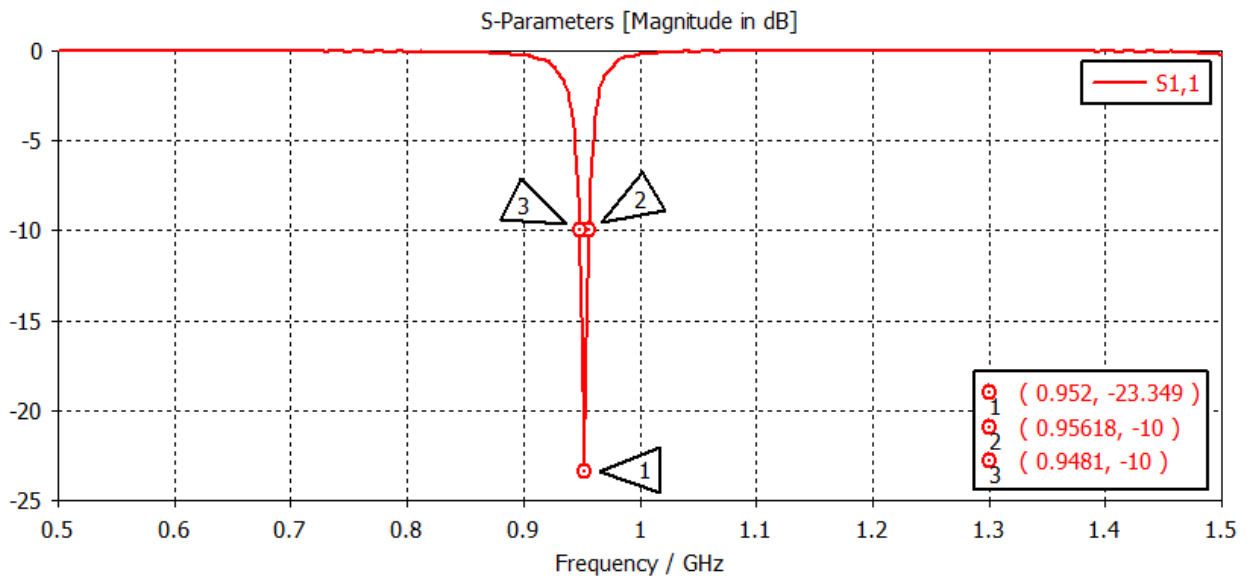**Figure 4.1: Geometry of the basic patch antenna.**

Figure 4.2: S$_{11}$ simulation of the theoretical patch antenna

By looking at the S_{11} of this antenna it is observed that it is about -23 dB at 952 MHz and the antenna achieves a realized gain of 5.23dB as shown in figure 4.3 and a narrow bandwidth.
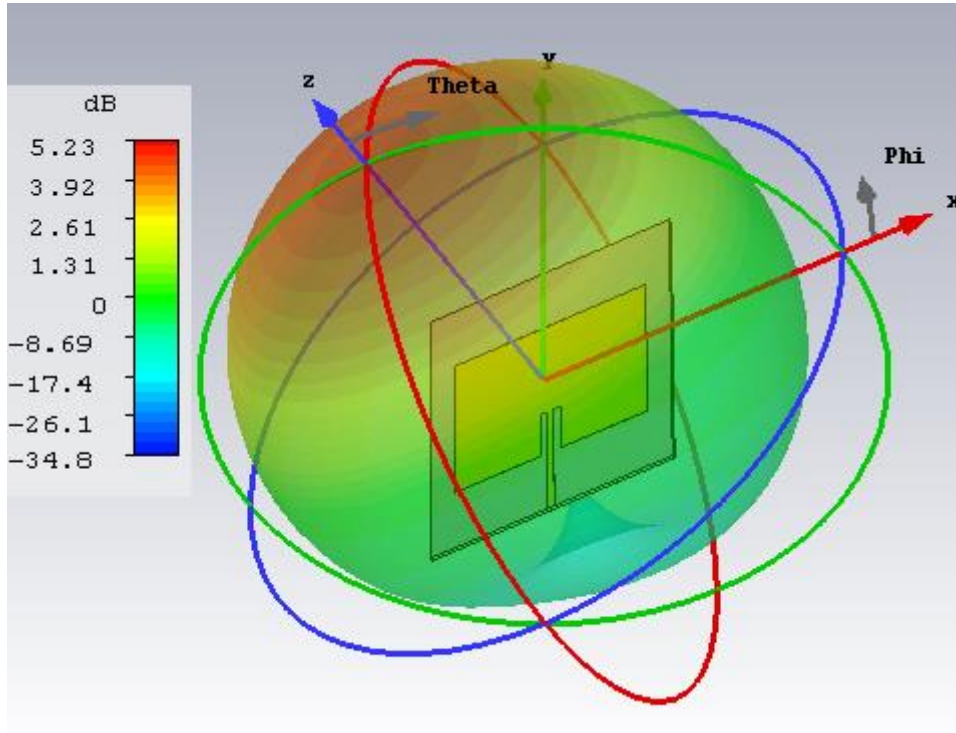

Figure 4.3: antenna gain and far field plot

4.3.1.1 Array for Microstrip Patch Antenna with Inset Feed

We used the same values of height of the dielectric substrate (h) and the same dielectric material at the design frequency and also the same dimension of single patch antenna. Figure 4.4 presents the structure of the array. The widths of the microstrip lines with Z_1 = 50 Ω and Z_2= 100 Ω are Wf1=1.33 mm and Wf= 3.21 mm, respectively and the lengths are Lf=10mm and Lf1=34mm.
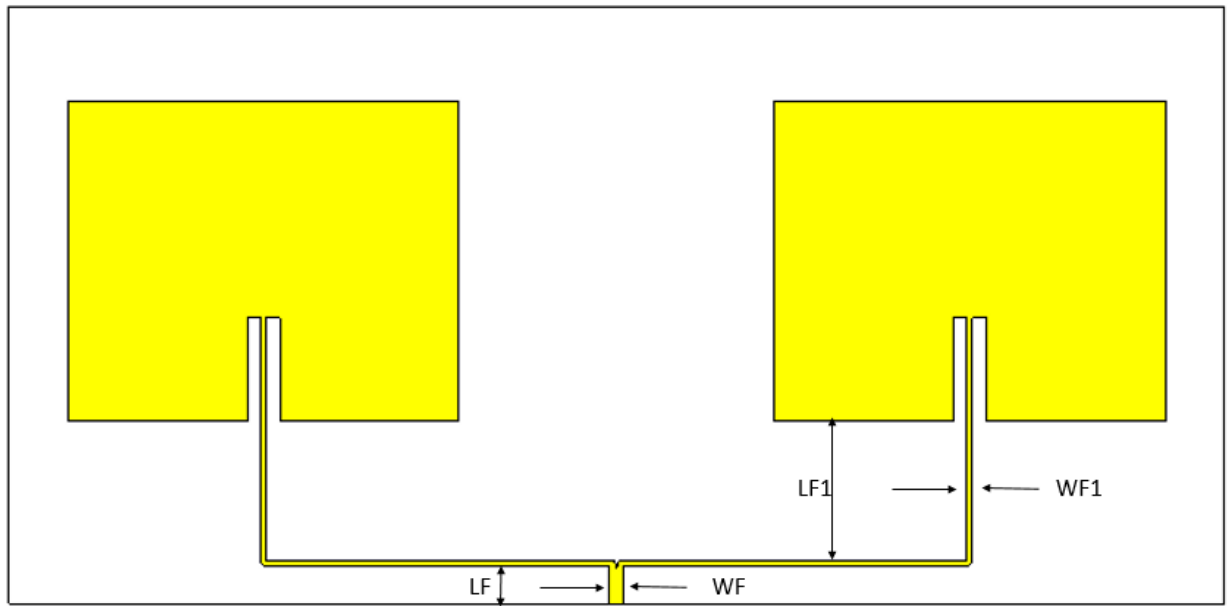
Figure 4.4: geometry inset-fed antenna array.

This array design achieves return loss S_{11} (-25.114 dB) at 951 MHz as shown in figure 4.5 with a realized gain of 7.88 dB in the far field region shown in figure 4.6 and it seems suitable to collect electromagnetic wave for energy harvesting.
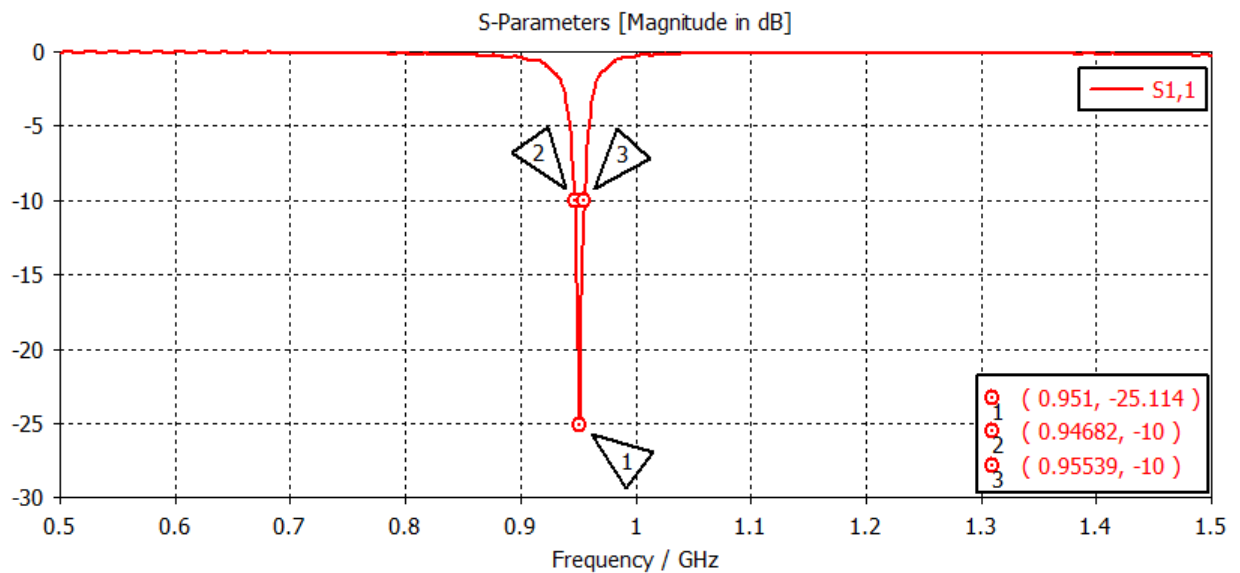

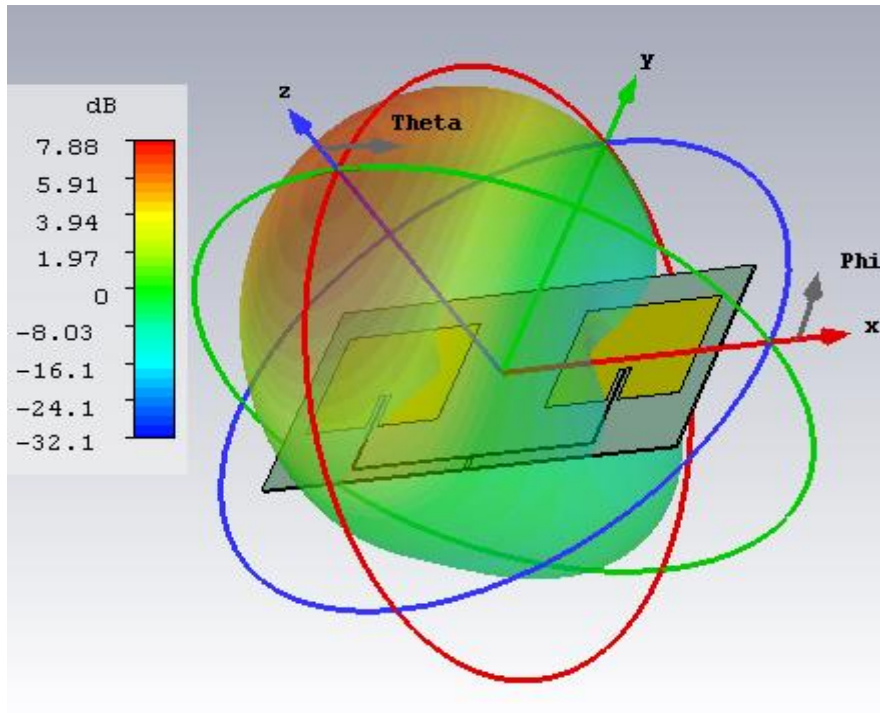**Figure 4.5: S_{11} for the inset-fed antenna array.**

Figure 4.6: far field gain of the inset-fed antenna array.

4.4 Design of the Rectifier

Figure 4.7 shows the design of the rectifier circuit constructed from a seven-stage voltage double circuit. This circuit contains: matching circuit, rectifier circuit and a resistor load.
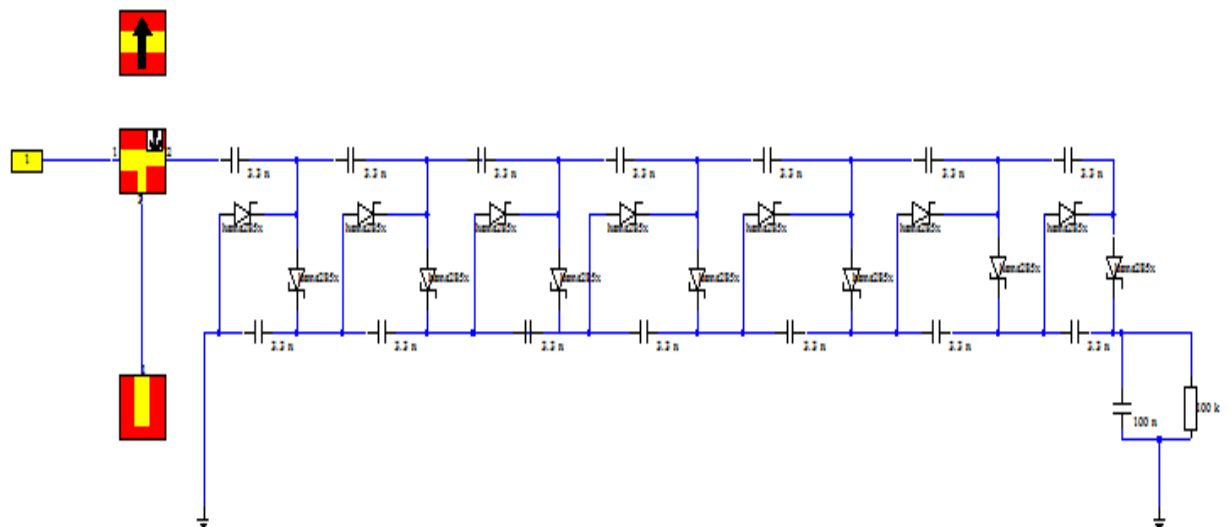

Figure 4.7: seven- stage voltage doublers using schottky diode HSMS 285X.

Matching circuit is placed between the source and the rectifier circuit to match the input impedance of and the rectifier to 50Ω.

Rectifier circuit contains two capacitors and two diodes in every stage. It is used to generate DC voltage of twice the peak amplitude of the input AC signal. Increasing the stages of rectifier will increase the output voltage of the circuit. Capacitors used here are 3.3 nF each capacitor.

The multiplier circuit utilizes a Schottky diode HSMS 285X as shown in Figure 3.6. The output voltage across the load decreases during the negative half cycle of the AC input signal. The voltage is inversely proportional to the product of resistance and capacitance across the load. Without the load resistor in the circuit, the voltage would be held indefinitely in the capacitor behaving like a DC signal, assuming ideal components. The capacitors are charged to the peak value of the input RF signal and discharged to the series resistance (Rs) of the diode. Thus the output voltage across the capacitor of the first stage is approximately twice that of the input signal. As the signal swings from one stage to another, there is an additive resistance in the discharge path of the diode and increase of capacitance due to the stage capacitors [13].

The matching circuit used here is the single stub matching. The simulated response of the circuit in Figure 4.7 is depicted in Figure 4.8 that clearly shows matching is achieved at frequency 951 MHz. The layout of the matching circuits shown in figure 4.9.
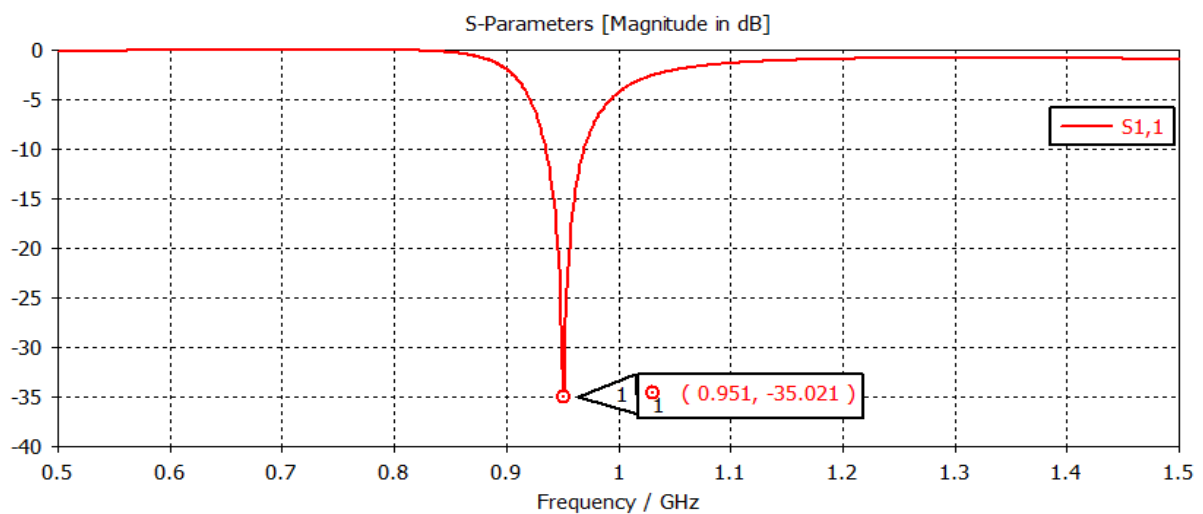

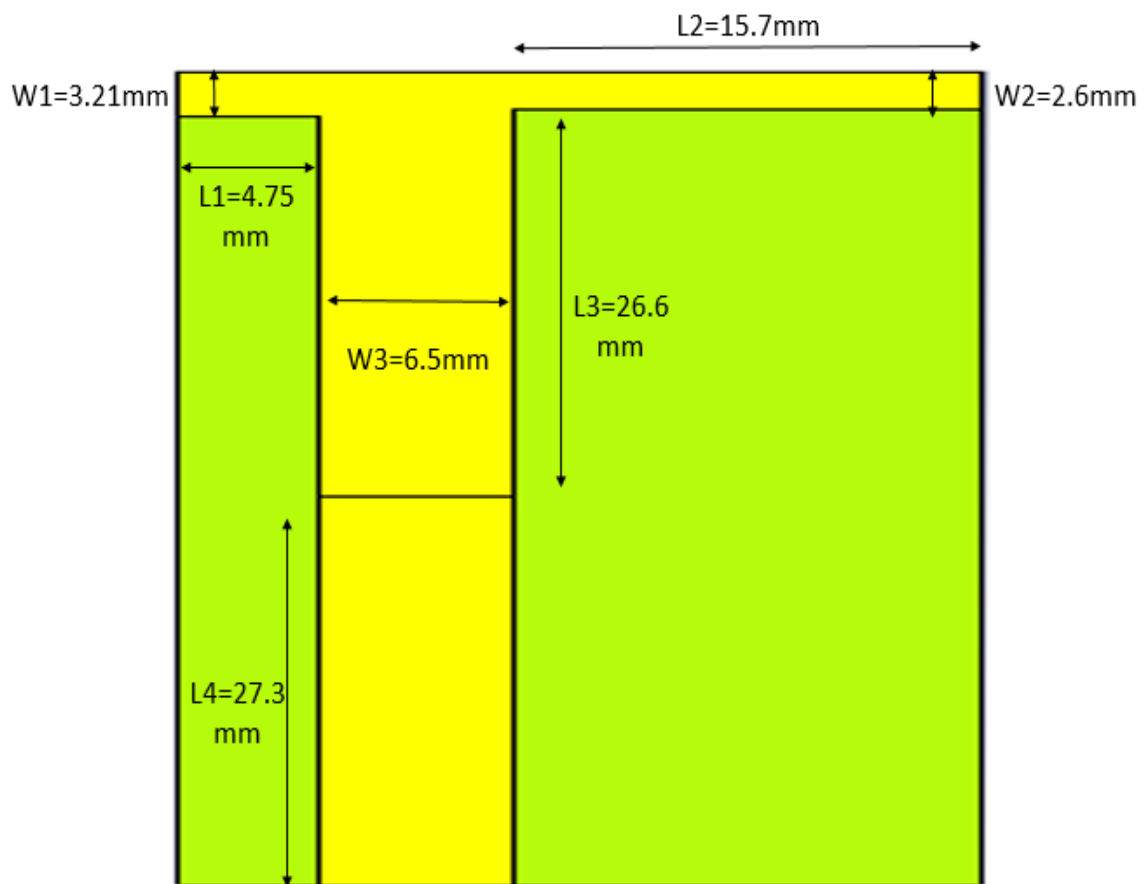**Figure 4.8: response of matching circuits**

Figure 4.9: matching circuit layout for seven stage rectifier

For rectifier simulations, we used the Multisim 13.0 software to determine the output voltage. In the simulation, the input power is varied from -20dBm to 20 dBm and the output load voltage is noted. As for the measurement a result, the rectifier circuit is injected with similar varies input power and the output load voltage is recorded using voltmeter. Figure 4.10 show the rectifier circuits design by Multisim 13.0 software and the simulated output DC power is 2.283 volt.
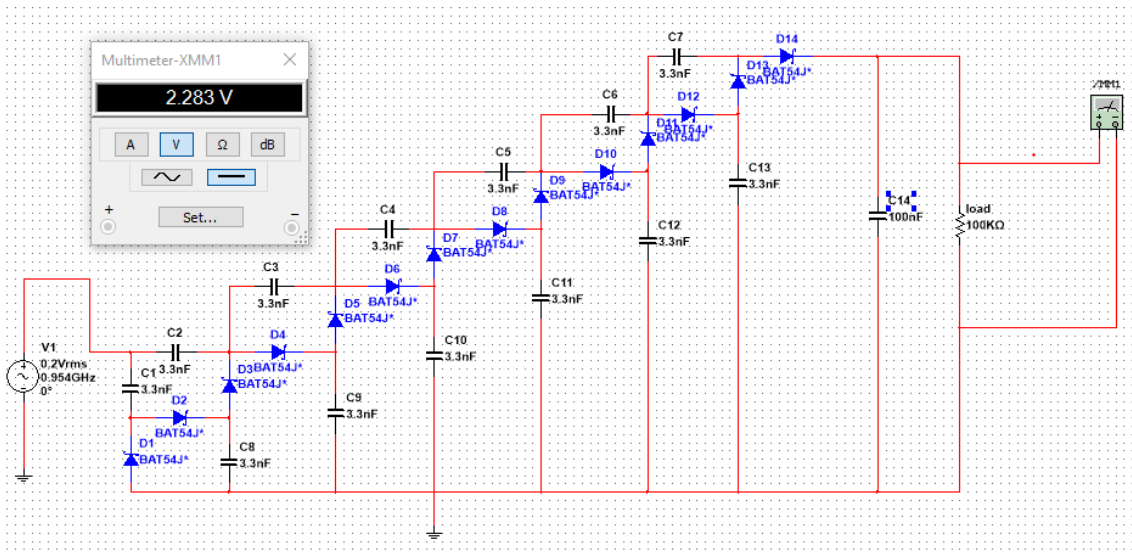
Figure 4.10: Rectifier design with multisim and output voltage.

4.5 Rectifier Fabrication

Because of unavailable component in the market due to siege, most of components are banned to enter the market here like the HSMS 2850 schottky diode and the double layer metal FR-4 substrate, we hardly get a component for single stage rectifier to fabricate. Hence we designed and simulated a single stage rectifier as shown figure 4.11 at the frequency 954 MHz and its response is shown in figure 4.12. Also the matching circuit layout which is an open stub for the single stage rectifier is shown in figure 4.13 with small changes in the parameters values compared to matching circuit of the seven stage rectifier. The values of c1 and c2 are 3.3nf and 100nf respectively, the load resistor is 100kΩ, the schottky diode parameters value shown in table 3.1.
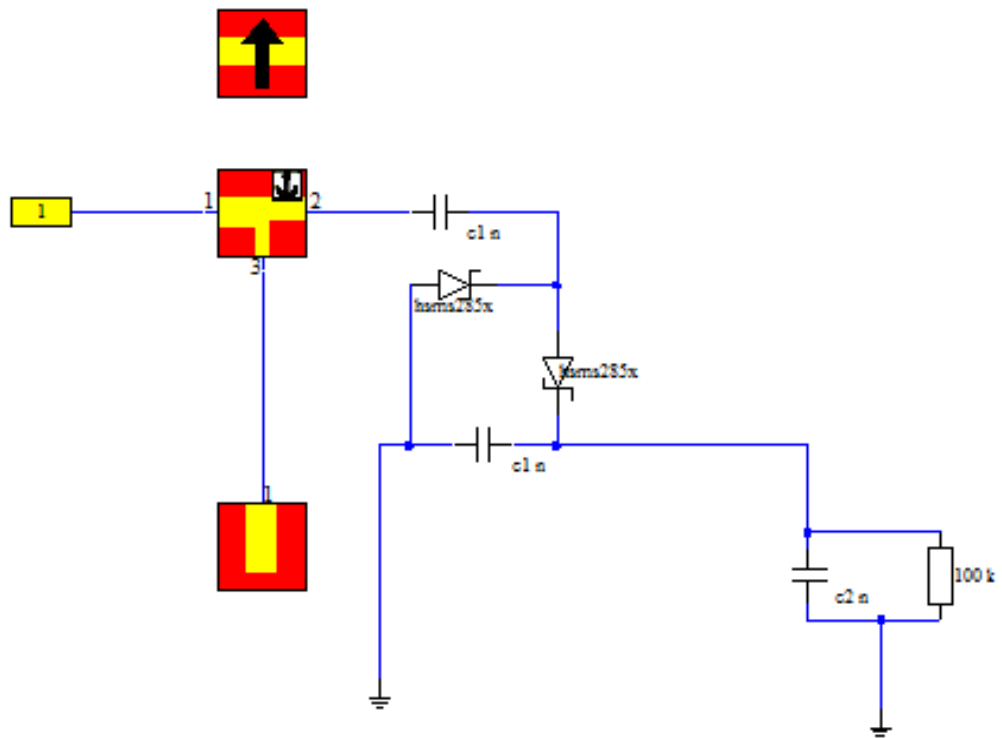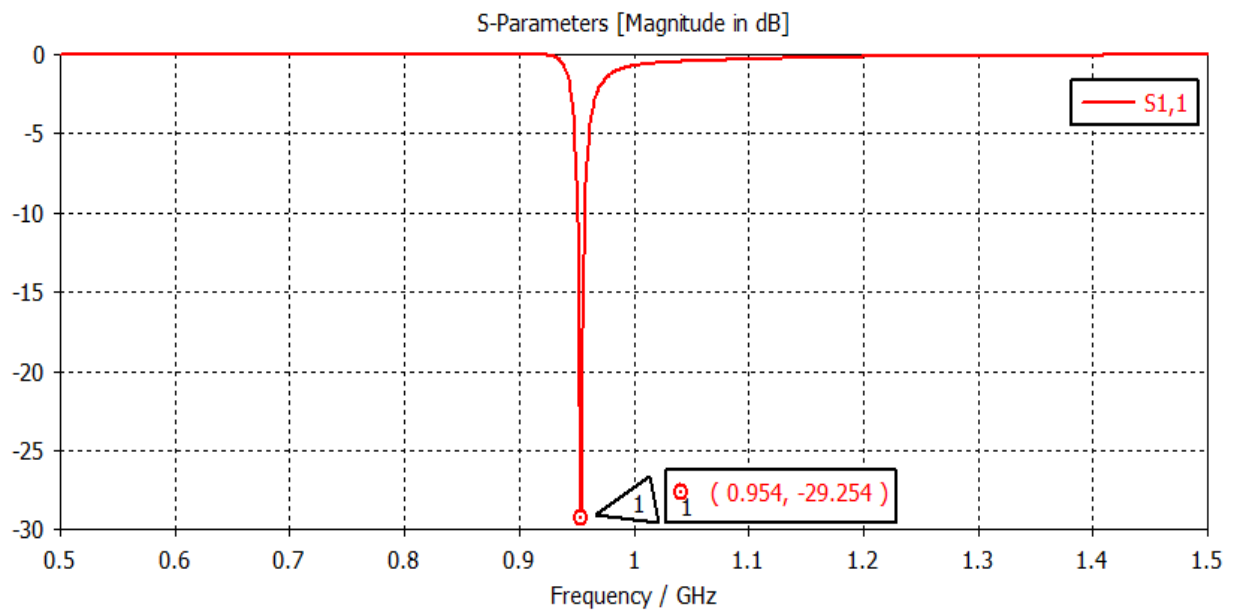
figure 4.11: single stage rectifier

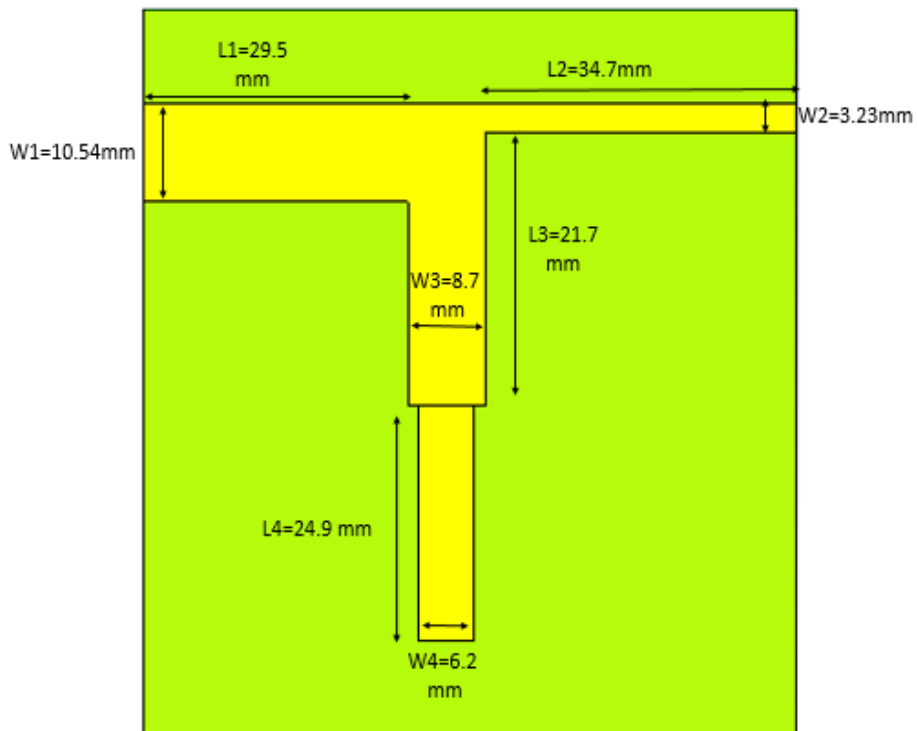**Figure 4.12: response of matching circuits for single stage**

figure 4.13: matching circuit layout for single stage

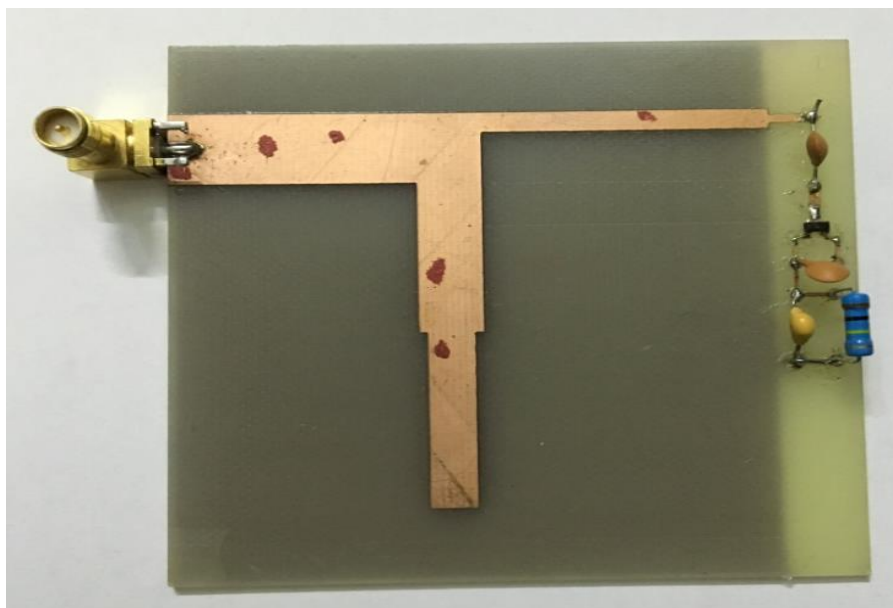The fabricated single stage rectifier with impedance matching circuit is shown in Figure 4.14.

figure 4.14: Fabricated single rectifier with impedance matching circuit

Due to unavailability of measurement equipment at the time for this work, particularly a network analyzer to test S_{11}, we were not able to test the circuit. Moreover, the designed antenna array has not been fabricated due to lack of FR-4 substrates. The circuit will be tested in the near future.

References

[1]   Y. Ren and C. Kai, "5.8-GHz Circularly Polarized Dual-Diode Rectenna and Rectenna Array for Microwave Power Transmission" IEEE Transactions on Microwave Theory and Techniques, VOL.54, NO.4, April2006

[2]   S. Alam, M. Sakib Ullah and S. Moury "Design of A Low Power 2.45 GHz RF Energy Harvesting Circuit for Rectenna" IEEE Transactions on Microwave Theory and Techniques,2013

[3]   F. Xie, G. Yang, and W. Geyi "Optimal Design of an Antenna Array for Energy Harvesting" IEEE Antennas and Wireless Propagation Letters, VOL.12, 2013
        [4] Y Suh and K. Chang, "A high-efficiency dual-frequency rectenna for 2.45 and 5.8-GHz wireless power transmission," Microwave Theory and Techniques, IEEE Transactions on, vol. 50, pp. 1784-1789, 2002.

[5]   S. Ladan, N. Ghassemi, A. Ghiotto, and K. Wu, "Highly Efficient Compact Rectenna for Wireless Energy Harvesting Application" IEEE microwave magazine, January2013.

[6]   S. Kumar, P. Patel, A. Mittal and A. De, "Design, Analysis and Fabrication of Rectenna for Wireless Power Transmission - Virtual Battery" IEEE, December 2012

[7]   H. Sun,Y. Guo,M. He,and Z. Zhong, "Design of a High-Efficiency 2.45GHz Rectenna for Low-Input-Power Energy Harvesting"IEEE Antennas and Wireless Propagation Letters, VOL.11, 2012.

[8]   E. M. Ali, N. Z. Yahaya, N. Perumal and M. A. Zakariya," Design and Development OF Harvester Rectenna at GSM Band for Battery Charging Application" ARPN Journal of Engineering and Applied Sciences, VOL. 10, NO 21, November, 2015.

[9]   G.Vignesh, U.Vairavan, P. Sunil Kumar & J.Senthil, S.Rajeswari, "RF Energy Harvesting" (IJARTET) International Journal of Advanced Research Trends in Engineering and Technology Vol. II, Special Issue XXV, April 2015.

[10]   M. Hosain, A. Kouzani. "Electromagnetic energy harvesting in a head mountable DBS device using a circular PIFA". International Conference on Complex Medical Engineering, 2013.

[11] J. Barak, H. Partal. "Efficient RF Energy Harvesting by using Multiband Microstrip Antenna Arrays with Multistage Rectifiers", Sub threshold Microelectronics Conference (SubVT), 2012 IEEE

[12] T. Mishra, S.K. Panda. "2.4GHz square slots antenna and power management circuit for wireless energy harvesting applications". 2012 IEEE Asia Pacific Conference on Antennas and Propagation, August 27-29, 2012, Singapore.

[13] Akter N., Hossain B., Kabir H., Bhuiyan A. H., Yeasmin M. and Sultana S., " Design and Performance Analysis of 10 Stage Voltage Doublers RF Energy Harvesting Circuit for Wireless Sensor Network". Journal of Communications Engineering and Networks,84-91,2014.

[14] C. Ratnaratorn, N.Wongsin, C.Mahatthanajatuphat, and P. Akkaraekthalin, "A Multiband Wide Slotted Antenna with Hilbert Fractal Slot on Rectangular Patch",IEEE,2013.

[15] P. Misra A. Tripathy, "A Novel Quad-band Printed Antenna Design using a Multi-Slotted Patch for Cellular Communication "International Journal of Computer Applications (0975 –8887) Volume 63– No.2, February 2013

.

5

Conclusion and Future Work

5.1 Conclusion

In this master thesis, the design of RF energy harvester using FR-4 substrate is investigated. For this purpose, different steps have been done. As a first step, A microstrip patch antenna with inset feed was simulated on FR-4 substrate with full ground plane using microwave studio CST software. It was chosen for power harvesting because it has a high directivity gain Furthermore an array antenna has been designed, it further increases the gain.

In the next Step, A seven stage rectifier based on voltage doubler is simulated by using the schottky diode specially HSMS-2850. The input RF signal to the rectifier is converted to DC voltage. The amount of output DC voltage depends on several parameters: number of stages, load and capacitors. In addition, the input impedance matching circuit was added, in order to transfer the maximum available power to the rectifier. The output DC voltage was measured by multisim software without matching circuit. For 0.2 V_{rms} input power at 954MHz, 2.283V is presented at the output of voltage doubler.

Finally, in the last step, one stage rectifier was connected to the matching circuits simulated and fabricated, Due to unavailability of measurement equipment at the time for this work, particularly a network analyzer to test S_{11}, we were not able to test the circuit. By studying this project, the band of antenna for energy harvesting application was successfully designed. The characteristics of the antennas have been studied. The rectifier circuit helps in converting the RF signal to output DC voltage. So by applying the energy harvesting system in the future it can enhance the lifetime of the low power devices and reduce the usage of the batteries.

5.2 Future Work

The future work related to this project will be fabrication of the simulated energy harvesting system and measurement of output DC voltage.

Moreover, more bands will be considered in future design to capture more energy.

Rectenna's for dual will be designed and fabricated on flexible substrates for the antenna like paper and textile. These materials give us the chance to make our antenna low profile, and conformal.

Finally, we still have to make some indoor measurements to test the work range of our system.

Appendix A

Surface Mount Zero Bias Schottky Detector Diodes

Technical Data

HSMS-2850 Series

Features

- Surface Mount SOT-23/ SOT-143 Packages
- Miniature SOT-323 and SOT-363 Packages
- High Detection Sensitivity: up to 50 mV/μW at 915 MHz
- Low Flicker Noise: -162 dBV/Hz at 100 Hz
- Low FIT (Failure in Time) Rate*
- Tape and Reel Options Available
- Matched Diodes for Consistent Performance
- Better Thermal Conductivity for Higher Power Dissipation

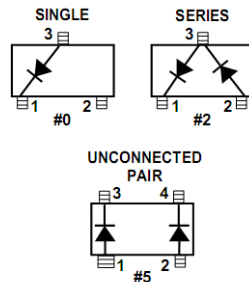* For more information see the Surface Mount Schottky Reliability Data Sheet.

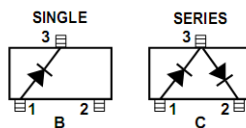## Pin Connections and Package Marking
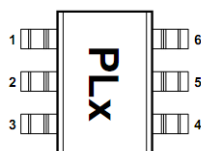
Notes:
1. Package marking provides orientation and identification.
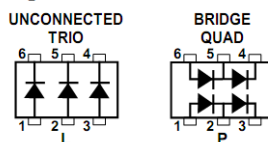2. See "Electrical Specifications" for appropriate package marking.

SOT-23/SOT-143 Package Lead Code Identification (top view)

SOT-323 Package Lead Code Identification (top view)

SOT-363 Package Lead Code Identification (top view)

Description

Agilent's HSMS-285x family of zero bias Schottky detector diodes has been designed and optimized for use in small signal ($P_{in} < -20$ dBm) applications at frequencies below 1.5 GHz. They are ideal for RF/ID and RF Tag applications where primary (DC bias) power is not available.

Important Note: For detector applications with input power levels greater than –20 dBm, use the HSMS-282x series at frequencies below 4.0 GHz, and the HSMS-286x series at frequencies above 4.0 GHz. The HSMS-285x series IS NOT RECOMMENDED for these higher power level applications.

Available in various package configurations, these detector diodes provide low cost solutions to a wide variety of design problems. Agilent's manufacturing techniques assure that when two diodes are mounted into a single package, they are taken from adjacent sites on the wafer, assuring the highest possible degree of match.

SOT-23/SOT-143 DC Electrical Specifications, T_C = +25°C, Single Diode

Part Number HSMS-	Package Marking Code[1]	Lead Code	Configuration	Maximum Forward Voltage V_F (mV)		Typical Capacitance C_T (pF)
2850 2852 2855	P0 P2 P5	0 2 5	Single Series Pair [2,3] Unconnected Pair [2,3]	150	250	0.30
Test Conditions				I_F = 0.1 mA	I_F = 1.0 mA	V_R = –0.5 V to –1.0V f = 1 MHz

Notes:
1. Package marking code is in white.
2. ΔV_F for diodes in pairs is 15.0 mV maximum at 1.0 mA.
3. ΔC_T for diodes in pairs is 0.05 pF maximum at –0.5 V.

SOT-323/SOT-363 DC Electrical Specifications, T_C = +25°C, Single Diode

Part Number HSMS-	Package Marking Code[1]	Lead Code	Configuration	Maximum Forward Voltage V_F (mV)		Typical Capacitance C_T (pF)
285B 285C 285L 285P	P0 P2 PL PP	B C L P	Single [2] Series Pair [2,3] Unconnected Trio Bridge Quad	150	250	0.30
Test Conditions				I_F = 0.1 mA	I_F = 1.0 mA	V_R = 0.5 V to –1.0V f = 1 MHz

Notes:
1. Package marking code is laser marked.
2. ΔV_F for diodes in pairs is 15.0 mV maximum at 1.0 mA.
3. ΔC_T for diodes in pairs is 0.05 pF maximum at –0.5 V.

RF Electrical Specifications, T_C = +25°C, Single Diode

Part Number HSMS-	Typical Tangential Sensitivity TSS (dBm) @ f = 915 MHz	Typical Voltage Sensitivity γ (mV/μW) @ f = 915 MHz	Typical Video Resistance RV (KΩ)
2850 2852 2855 285B 285C 285L 285P	–57	40	8.0
Test Conditions	Video Bandwidth = 2 MHz Zero Bias	Power in = –40 dBm R_L = 100 KΩ, Zero Bias	Zero Bias

Absolute Maximum Ratings, T_C = +25°C, Single Diode

Symbol	Parameter	Unit	Absolute Maximum[1]	
			SOT-23/143	SOT-323/363
P_{IV}	Peak Inverse Voltage	V	2.0	2.0
T_J	Junction Temperature	°C	150	150
T_{STG}	Storage Temperature	°C	-65 to 150	-65 to 150
T_{OP}	Operating Temperature	°C	-65 to 150	-65 to 150
θ_{jc}	Thermal Resistance[2]	°C/W	500	150

Notes:
1. Operation in excess of any one of these conditions may result in permanent damage to the device.
2. T_C = +25°C, where T_C is defined to be the temperature at the package pins where contact is made to the circuit board.

ESD WARNING:
Handling Precautions Should Be Taken To Avoid Static Discharge.

Equivalent Linear Circuit Model
HSMS-285x chip
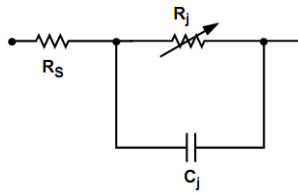
R_S = series resistance (see Table of SPICE parameters)

C_j = junction capacitance (see Table of SPICE parameters)

$R_j = \dfrac{8.33 \times 10^{-5}\, nT}{I_b + I_s}$

where
I_b = externally applied bias current in amps
I_s = saturation current (see table of SPICE parameters)
T = temperature, °K
n = ideality factor (see table of SPICE parameters)

Note:
To effectively model the packaged HSMS-285x product, please refer to Application Note AN1124.

SPICE Parameters

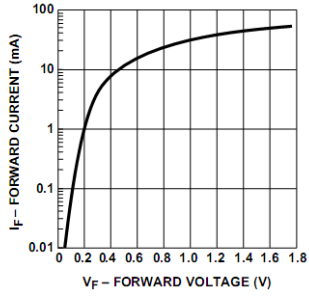| Parameter	Units	HSMS-285x
B_V	V	3.8
C_{J0}	pF	0.18
E_G	eV	0.69
I_{BV}	A	3 E-4
I_S	A	3 E-6
N		1.06
R_S	Ω	25
P_B (V_J)	V	0.35
P_T (XTI)		2
M		0.5

Typical Parameters, Single Diode

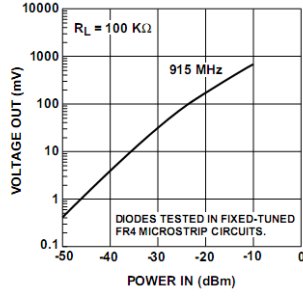Figure 1. Typical Forward Current vs. Forward Voltage.

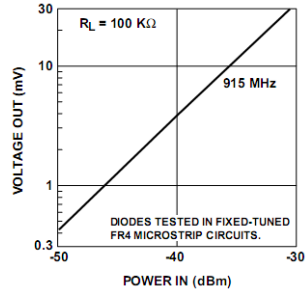Figure 2. +25°C Output Voltage vs. Input Power at Zero Bias.
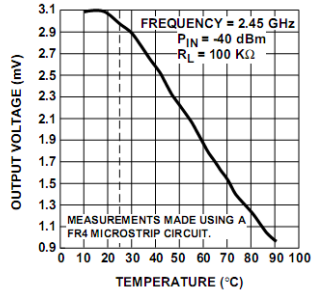

Figure 3. +25°C Expanded Output Voltage vs. Input Power. See Figure 2.

Figure 4. Output Voltage vs. Temperature.